

國立交通大學

電信工程研究所

博士論文

具有可調 Q 共振器之超寬頻平面帶
拒單極天線分析與設計

Modeling and Design of Planar Band-notched
UWB Monopole Antenna with Tunable-Q
Resonators

研究生：吳松融

指導教授：唐震寰 教授

中華民國九十九年七月

具有可調Q共振器之超寬頻平面帶拒單極天線分
析與設計

Modeling and Design of Planar Band-notched UWB Monopole
Antenna with Tunable-Q Resonators

研究生：吳松融

Student : Sung-Jung Wu

指導教授：唐震寰 博士

Advisor : Dr. Jenn-Hwan Tarng

國立交通大學

電信工程研究所

博士論文



A Dissertation

Submitted to Institute of Communication Engineering
College of Electrical and Computer Engineering
National Chiao Tung University
in partial Fulfillment of the Requirements
for the Degree of Doctor of Philosophy in
Communication Engineering
Hsinchu, Taiwan, Republic of China

中華民國九十九年七月

具有可調 Q 共振器之超寬頻平面帶 拒單極天線分析與設計

學生：吳松融

指導教授：唐震寰

國立交通大學電信工程研究所 博士班



本篇論文主旨在於實現適用於超寬頻無線通訊系統之平面帶拒天線，其天線結構為叉子形狀之平面超寬頻天線(fork-shaped UWB antenna)與四種新型諧振單元(resonator)。首先，本文提出一種具有叉子形狀之平面超寬頻天線，其操作頻率為 3.1GHz ~ 10.6GHz 並具有全方向性的場型、平坦的增益頻率響應及易於製作的特性，而四種可以應用在超寬頻天線的新型諧振單元分別為 tapped-line coupled resonator, square-looped resonator, end-coupled resonator 和 open-looped resonator。本論文即探討這些諧振單元與超寬頻天線之整合與最佳化，有別於一般利用四分之一波長槽線(slot)或微帶線(strip)與天線形成共振結構之超寬頻帶拒天線，本論文所提出的超寬頻平面帶拒天線明顯地改善帶拒效果，其帶拒頻率和增益抑制效果分別為 5-6GHz 和 15-30dB。除了提出天線結構上的創新，本論文也提出一種將超寬頻平面帶拒天線等效成一集總元件電路(lump circuit)的方法，利用該方法所得到的阻抗響應和 HFSS 模擬軟體的模擬結果有相當的一致性。

Modeling and Design of Planar Band-notched UWB Monopole Antenna with Tunable-Q Resonators

Student : Sung-Jung Wu

Advisor : Dr. Jenn-Hwan Tarn

Institute of Communication Engineering
National Chiao Tung University

ABSTRACT

Since the Federal Communication Commission (FCC) allowed unlicensed use of 3.1-10.6 GHz unlicensed band and EIRP less than -41.3dBm/MHz for Ultra-wideband (UWB) communication, UWB technology has been widely investigated and developed for short range wireless applications. However, the exiting wireless local area network (WLAN) is used in 5-6 GHz and interferes with UWB performance such as sensitivity and signal-to-noise ratio. This dissertation is devoted to manifest and analyze new categories of resonators used in UWB antenna to achieve band-notched performance. A fork-shaped UWB antenna is firstly designed for wide bandwidth, omni-directional pattern and flat gain response over 3.1-10.6GHz. Then, four kinds of resonators, i.e., tapped-line coupled resonator, square-looped resonator, end-coupled resonator and open-looped resonator, are designed and used respectively in a fork-shaped UWB antenna to create a notched band. Moreover, the schematic equivalent circuit of each resonator are investigated and discussed along with band-notched performance. The proposed antennas feature flat gain frequency response, small varied group delay and 10 to 25 dB gain suppression in the notched band. Then, an equivalent circuit model illustrates the band-notched behaviors more clearly. The antenna input admittance calculated with the equivalent circuit model reasonably agrees with the HFSS simulated result. Accordingly, the band-notched antenna can effectively select target bands by adjusting these antenna parameters. The purpose of this study provides high performance antennas which is suitable for UWB applications.

謝誌

本論文得以如期順利完成，首先要感謝指導教授唐震寰博士的耐心栽培與指導，其嚴謹的教學精神與研究態度，不僅使學生在專業知適合研究工作上獲益良多，待人處世方面亦成長許多，師恩浩瀚，在此獻上最誠摯的感謝。另外，口試委員彭松村教授、楊成發教授、林丁丙教授、黃瑞彬教授及鍾世忠教授在口試期間的指導以及對本論文提出許多改進的地方，均使學生獲益良多，亦使本論文更為完善，僅此表達謝意。

研究過程中，特別要感謝文崇、瑞榮、維儒學長的指導與提供的寶貴意見，學弟耿賢、鈺宏和美麗的梁麗君小姐幫忙處理許多計畫事情讓我得以專心於學術上的研究；此外，學弟俊諺、雅仲、振銘、廣琪、兆凱、明宗、冠豪、國政、佳迪、昌喆、詠順的熱心協助與討論，使我受益良多。另外也要感謝我的朋友、中偉、金鋒、人慶、冠集、文清、政軒、小馬、小黑、皓亮、剛名，增添我許多生活上的樂趣。特別感謝剛名這一路上陪我喝酒談心聊天的，陪我度過無數的夜晚。

最後也是最重要的，特別感謝家人的支持與鼓勵，我的雙親吳昌先生、周秀菊女士從小就給予我良好的學習環境，最佳的成長環境，姐姐貞儀和一雙可愛的兒女冠辰和旨芸給予我最溫馨的關懷，妹妹附儒、弟弟宗樺給我精神上對大的支持，以及怡蓁給我的支持與鼓勵，很自豪的說：沒有你的認真付出，就沒有今天的松融，我願把我所有的一切都與你分享。最後我要將此份榮耀獻給我最親愛的家人。

吳松融

民國 99 年 7 月 新竹

Chapter List

1	Introduction	1
1.1	Research motivation	1
1.2	Literature survey	4
1.3	Contributions	7
1.4	Chapter outline	10
2	Fundamental theory and Architecture of Proposed Antenna.....	12
2.1	Foster canonical forms and dimensionless normalized antenna transfer function for UWB antenna.....	13
2.2	A Band-Notched UWB Planar Monopole Antenna with Tapped-Line Coupled Resonator	18
2.2.1	Geometry and design concept.....	18
2.2.2	Design guideline and performance	21
2.3	Summary	28
3	Planar Band-Notched UltraWideband Antenna with Square-Looped or End-Coupled Resonator.....	30
3.1	Geometry and Design Guideline	32
3.1.1	Geometry of the proposed antenna	32
3.1.2	Square-looped resonator and End-coupled resonator	34
3.2	The performance of fork-shaped UWB antenna with square-looped resonator ..	38
3.2.1	Parametric Study.....	40
3.2.2	Radiation Patterns, Gain response and Group Delay	43
3.1	Summary	46
4	An UltraWideband Monopole Antenna with a Band-Notched Open-Looped Resonator	48
4.1	Antenna Configuration and Performance.....	50
4.2	Effect of Resonator on Notched Bands.....	56

4.3	The Equivalent Circuit Model.....	62
4.4	Gain response and Group Delay	68
4.5	Summary	70
5	Conclusion.....	72
5.1	Conclusion	73
5.2	Future Work	74
6	Reference.....	76



Figure List

Fig. 2.1 Forster canonical forms (a) electric antenna model (b) magnetic antenna model.	14
Fig. 2.2 Schematic diagram of the arrangement for measuring the system transfer function.	15
Fig. 2.3 Configuration of the proposed antenna. (a) Top view. (b)The proposed resonator.	19
Fig. 2.4 Simulated and measured return loss of the proposed antenna.	20
Fig. 2.5 Simulated return loss at various lengths of the resonator.	21
Fig. 2.6 Simulated return loss at the various feeding locations of resonator at antenna.	22
Fig. 2.7 Measured and Simulated radiation patterns at (a) 4GHz. (b) 7GHz. (c) 10GHz. (Unit:dBi).....	23
Fig. 2.8. Measured gain response of the proposed antenna. at $\theta=0^\circ$, $\theta=90^\circ$, $\theta=180^\circ$, $\theta=-90^\circ$	24
Fig. 3.1. Geometry of proposed antenna.....	33
Fig. 3.2. Measured and simulated VSWR of fork-shaped UWB antenna with square-looped resonator.....	34
Fig. 3.3 (a) Square-looped resonator structure; (b) Tapped-line coupled resonator.....	35
Fig. 3.4 Schematic equivalent circuit of square-looped resonator.	36
Fig. 3.5 Admittances of the proposed antenna.	36
Fig. 3.6 (a) End-coupled resonator structure (b) Schematic equivalent circuit of end-coupled resonator.....	37
Fig. 3.7 Measured and simulated VSWR of the fork-shaped UWB antenna with end-coupled resonator.	38
Fig. 3.8 Simulated current distribution of the proposed antenna at 5.5 GHz.(a) square-looped resonator. (b) end-coupled resonator.	39
Fig. 3.9 VSWR versus the various lengths of the square-looped resonator.	40
Fig. 3.10 VSWR versus the various input positions of the square-looped resonator.....	41
Fig. 3.11 VSWR versus the various positions of the resonator in the x-oriented.	42
Fig. 3.12 Measured and Simulated radiation patterns at (a) xy-plane. (b) xz-plane. (c) yz-plane. (Unit:dBi).....	43
Fig. 3.13 Measured gain response (a) $\theta = 0^\circ$, $\theta = 90^\circ$, $\theta = 180^\circ$, $\theta = 270^\circ$. (b) $\theta = 45^\circ$, $\theta = 135^\circ$, $\theta = -45^\circ$, $\theta = -135^\circ$	45

Fig. 3.11 Measured and Simulated radiation patterns at (a) xy-plane. (b) xz-plane. (c) yz-plane. (Unit:dBi).....	45
Fig. 4.1 Configuration of the proposed antenna. (a)Top view. (b) Proposed resonator. (c) Schematic equivalent circuit model of proposed resonator.....	51
Fig. 4.2 Measured and simulated return loss of proposed antenna.....	54
Fig. 4.3 Simulated return loss of various ground plane sizes.	54
Fig. 4.4. Measured and Simulated radiation patterns at (a) xz-plane. (b) yz-plane. (c) xy-plane. (Unit:dBi).....	55
Fig. 4.5 Simulated return loss of various folded lengths of the resonator. ..	57
Fig. 4.6 Simulated return loss of various positions of the tapped-line.	58
Fig. 4.7 Simulated return loss according to various vertical position of resonator at the antenna.	60
Fig. 4.8 Simulated return loss according to various horizontal positions of resonator at the antenna.	61
Fig. 4.9 (a) Exact structure of the proposed resonator. (b) One-port lump equivalent circuit network of the proposed resonator. (c) Two-port lump equivalent circuit network of the proposed resonator. (d) Simplified equivalent circuit model of the proposed antenna.	63
Fig. 4.10 Compared results between HFSS and the simplified equivalent circuit. (a) Simulated impedance of the resonator. (b) Simulated admittance of the proposed antenna.....	67
Fig. 4.11 Measured gain response of the proposed antenna. (a) $\theta = 0^\circ$, $\theta = 90^\circ$, $\theta = 180^\circ$, $\theta = -90^\circ$. (b) $\theta = 45^\circ$, $\theta = 135^\circ$, $\theta = -135^\circ$, $\theta = -45^\circ$	69
Fig. 4.12 Measured group delay of the proposed antenna.	70

1 Introduction

1.1 Research motivation

With the growing demand for wireless communication, wireless technologies such as 2G/3G cellular phone, global positioning system (GPS), wireless local area network (WLAN), and wireless personal area network (WPAN) have been developed at a fast pace during the past decades. In these technologies, the goal of WPAN is personal multimedia wireless transmission with much higher data rate but shorter transmission range in the indoor environment. It also complements the other technologies to satisfy the diverse demands of wireless communication. The UWB technology is one of the WPAN technologies and it attracts considerable attentions in the literature. The main difference between UWB technology and other technologies is the operating bandwidth.

TABLE 1.1

FCC assigned spectra for UWB application

Surveillance systems	1.99-10.6 GHz
Medical systems	3.1-10.6GHz
Through-wall imaging systems	<960MHz ; 1.99-10.6GHz
Communication and measurement systems	3.1-10.6GHz
Vehicular radar systems	22-29GHz

TABLE 1.2

FCC indoor emission mask for UWB communication system

Frequency in MHz	EIRP in dBm
960-1610	-75.3
1610-1990	-53.3
1990-3100	-51.3
3100-10600	-41.3
Above 10600	-51.3

The bandwidth of UWB is 7.5 GHz (from 3.1GHz to 10.6GHz), while bandwidth of other technologies such as 2/3G and WLAN are just several MHz. Furthermore, since the Federal Communication Commission (FCC) has allowed unlicensed use of 3.1-10.6 GHz unlicensed band with EIRP less than -41.3dBm/MHz for Ultra-wideband (UWB) communication, UWB technology has been widely investigated and developed for short range wireless applications[1][2]. FCC regulated essential emissions and some applications are briefly shown in Table. 1.1 and 1.2, respectively. In addition, the FCC has also redefined the bandwidth of UWB signal i.e., fractional bandwidth is greater 20% or occupied bandwidth is greater than 500MHz on a 10 dB return loss level. Compared with narrow band systems, the UWB technology has better system performance including high resolution radar imaging, rejection of multipath cancellation effects, and transmission of high data rate signals because of its extremely wide bandwidth [3]-[4].

The UWB systems can be divided into two categories: direct sequence UWB (DS-UWB) and multiband orthogonal frequency division multiplexing (MB-OFDM). The DS-UWB proposal foresees two different carrier frequencies at 4.104(low band) and 8.208 GHz (high band). The DS-UWB is operated by utilizing a several GHz bandwidth and transmitting sub-nanosecond pulse. The MB-OFDM divides the 13 sub-intervals into the allocated spectrum and transmits much broader pulse. According to the MB-OFDM format in 802.15.3a, each bandwidth of sub-interval is 528MHz.

However, the exiting wireless local area network (WLAN) is used in 5-6 GHz and interferes with the UWB operation. The interference from nearby communication system degrades the system performance such as sensitivity and signal-to-noise ratio. Hence, UWB system needs to reject the interferences of existing wireless networking technologies such as IEEE 802.11a in the U.S. (5.15–5.35 GHz, 5.725–5.825 GHz) and HIPERLAN/2 in Europe (5.15–5.35 GHz, 5.47–5.725 GHz). The UWB system uses extra band-stop filters to suppress dispensable bands in some applications. Nevertheless, the use of filters increases the complexity of UWB system, which leads to an increase in cost. Several literatures propose the UWB antenna with filtering property in 5-6GHz, therefore extra band-stop filter is not required in the system. Thus, the UWB antenna not only requires wide impedance matching, stable radiation characteristics, compact size, and low manufacturing cost but also provides the notched band to minimize the potential interferences.

This dissertation is devoted to manifest and analyze new categories of resonators used in UWB antenna to achieve band-notched performance. Various types of resonators with fork-shaped UWB antenna are thoroughly investigated and analyzed. The purpose of this study provides high performance antennas which is suitable for UWB applications.

1.2 Literature survey

Many studies have been proposed an extreme broadband antenna for UWB radio systems [5]-[19]. Abbosh *et al.* discussed the performances of UWB planar monopole

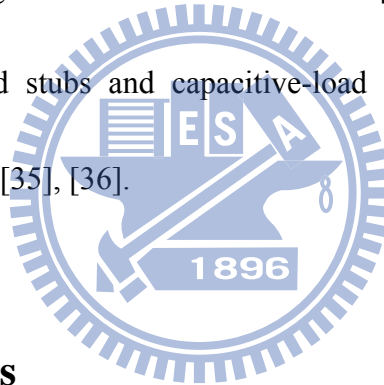
antennas with a circular or elliptical shape [14]. Chen *et al.* discussed ground plane effect on a small print UWB antenna [15]. Cheng *et al.* proposed a compact and low profile printed wide-slot inverted cone antenna for UWB applications [16]. Low *et al.* described a UWB suspended plate antenna (SPA) with enhanced impedance and radiation performance [18].

These UWB antennas have to operate across a very wide bandwidth with consistent polarization, radiation patterns, gain response and group delay. A number of technologies have been proposed for wide-band impedance matching. Initially, the traveling wave concept is extensively applied to slot and bowtie type antennas in order to utilize wide bandwidth and omni-radiation patterns [20]-[22]. However, these antennas usually have inherently larger size and need a larger ground plane. To overcome this problem, many researchers propose the aperture antenna. The advantages of aperture antennas are bandwidth enhancement and easy to be integrated with RF circuit for low cost manufacturing [20],[23]. In aperture antenna design, the antenna usually consists of a widened slot/aperture and an exciting stub. The bandwidth of aperture antenna, especially for the low frequency, is determined by the size of the exciting stub and the distance between the exciting stub and the edge of the aperture. In addition, the monopole antenna with flat structure is the most popular UWB antenna because of its light weight, low cost and ease of fabrication. The monopole antenna with various shapes, such as circle, triangle and ellipse, brings about broad bandwidth operation and has compact antenna and ground size [24]-[26].

The exiting wireless local area network (WLAN) is used in 5-6 GHz and may interfere with the UWB operation. Therefore, the UWB system uses extra band-stop filters to suppress dispensable bands in some applications. Nevertheless, the use of filters increases the complexity of UWB system, which leads to an increase in cost. Several literatures propose the UWB antenna with filtering property in 5-6GHz for removing the requirement of extra band-stop filter in the system [27],[28]. Several researchers have created transmission zero at the required notched bands by introducing associated resonators in the antenna. By placing the resonator in the antenna, the antenna impedance shifts to a very high or very low level and brings out impedance mismatch at the notch band. Simultaneously, the antenna impedance at notched band is similar to the virtual-open or virtual-short circuit and is capable of not only preventing energy from transmitting to free space, but also avoiding receiving the unwanted signal from free space.

Researches in some literatures produce band-rejection characteristics by cutting a slot on the antenna [29]-[31] or adding a tuning metal stub within the antenna structure [23],[32]. The creating notched band method is the important issue of UWB antenna designs and can be categorized in three types. One is to cut the thin slit in the antenna structure [8]-[9]. Another is to add plastic strip in the aperture area of antenna or nearby radiator. The plastic strip and the part of antenna form a resonant structure which leads to a sudden impedance change in the notching frequency [27], [28]. The third method is to directly add the narrow-band resonator

in the antenna structure [6], [7], [34]. In the two former mentioned methods, the notched frequency is mainly determined by the length of slit/strip. These lengths usually proportion to (1) a half wavelength of notched frequency for both the short-end slit and open-end strip or (2) a quarter wavelength of notched frequency for open-end slit. Different from the two above-mentioned methods, the notching frequency and bandwidth of antenna mostly depend on the resonant frequency and quality factor of resonator, respectively. Qu *et al.* created a notched band by a coplanar waveguide resonant cell [33]. Zaker *et al.* used an H-shaped conductor-backed plane to generate band-notched effect [7]. Other resonator forms, such as folded strips, two T-shaped stubs and capacitive-load strips have also been applied for band-notching purposes [6], [35], [36].



1.3 Contributions

Although the resonators are well accepted in band-notched antenna design, band-notched antenna performance is sometimes quite limited owing to the structure of the antenna and resonator. Meanwhile, the return loss level at the notched band is also a crucial factor for estimating gain suppression. In general, the return loss level is simply in reverse proportion to the gain suppression of the antenna [5]-[7]. The following examples explain the limited performance. The first example is that the amount of gain suppression is around 20dB at specific angles, but the gain suppression is only several dB at $\theta = 0^\circ$ [7]. The next example

is that the bandwidth of the notched band on the 10 dB return loss condition is overlapped with wanted UWB operating frequency, i.e., the bandwidth of the notched band is unsatisfactory for UWB applications [5], [6].

Previous literatures have mainly focused on the band-notched UWB antenna for wide operating bandwidth and band-notched performance. The band-notched performance in these literatures could utilize three observed criteria to estimate notched band antenna performance, i.e., gain suppression, bandwidth and roll-off rate (frequency selectivity) of the notched band. These criteria strongly relate to the structure and quality factor of the resonator [5]-[7]. According to our knowledge and experiments, the resonator position at the antenna should be included in the notched-band antenna design because it is also related to band-notched performance. Hence, the quality factor and resonator position can be accommodated simultaneously to improve the controlled ability of the notched band.

This dissertation is devoted to realize and analyze a new category of band-notched UWB antenna used in various resonators. The specific contributions of the dissertation are summarized as follows:

(1) The band-notched UWB antenna using resonators are proposed. To investigate band-notched performance, the proposed antennas consist of a fork-shaped antenna and a resonator with high quality factor. The fork-shaped antenna is designed for wide operating range. The proposed resonator is placed at the center of the fork-shaped antenna, creating the

5-GHz notched band. Using this arrangement, this work emphasizes the resonator effects. The proposed antennas also show good performance, such as fast roll-off rate of return loss, 10-30dB gain suppression ability and narrow notched bandwidth at the notched band.

(2) The tapped-line coupled resonator, square-looped resonator, end-coupled resonators and open-looped resonator are designed for employing in the antenna. Compared to other band-notched methods, the proposed resonators have several advantages.

- The resonator is placed in the fork-shaped antenna center and does not affect the extra antenna size.
- The resonator only slightly interferes with fork-shaped antenna performance except within notched band.
- The resonator has simple geometry with fewer parameters, releasing computation load in the optimization process. The notched frequency is mainly determined by the resonator structure.
- The resonator demonstrates the good band-notched performances such as narrow notched bandwidth, fast roll-off rate as well as 10-30 dB gain suppression (in generally, the gain suppression of thin strip and plastic strip are usually less than 10dB [08]-[11]).

(3) The essential techniques for analyzing UWB antenna with a resonator are discussed. To quickly understand the proposed antennas, the equivalent circuit model is created. The

calculated antenna input impedance used in this equivalent circuit mode agrees with the full-wave simulation.

1.4 Chapter outline

The organization of dissertation is described below.

In chapter 2, the Forster canonical forms and the dimensionless normalized antenna transfer function for analyzing the performance of an UWB antenna are firstly presented. These techniques will be intensively used in the following sections. Finally, a notched-band UWB planar monopole antenna using the tapped-line coupled resonator is proposed and compared to UWB antennas in the literature.

In Chapter 3, a planar band-notched ultra-wideband (UWB) using a square-looped and an end-coupled resonator respectively is proposed. To obtain the 5-6 GHz WLAN notched band, both square-looped and end-coupled resonator are designed and placed at fork-shaped UWB antenna center. The characteristics and schematic equivalent circuit of each resonator are discussed. Parametric studies are analyzed to explore the antenna operating mechanism. Accordingly, the band-notched antenna can effectively select target bands by adjusting different resonator structures. The proposed antenna features flat gain frequency response, small varied group delay and 10 to 25 dB gain suppression in the notched band.

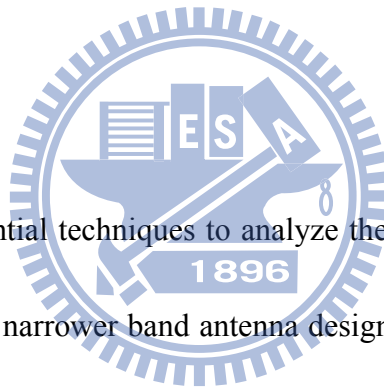
In Chapter 4, a novel band-notched planar monopole ultrawideband (UWB) antenna is proposed. A notched band, located in the 5 GHz WLAN band, is created using a resonator at

the center of a fork-shaped antenna. The resonator is composed of an open-looped resonator and two tapped lines. With the open-looped resonator, the antenna has a good band-notched performance and bandstop-filter-like response in the target band. A parametric study of the notched bandwidth is described that explored the antenna operating mechanism. Then, an equivalent circuit model illustrates the band-notched behaviors more clearly. The antenna input admittance calculated with the equivalent circuit model reasonably agrees with the HFSS simulated result. The proposed antenna also features flat gain frequency responses, small varied group delay and 15 to 35 dB gain suppression at the notched band. Accordingly, the band-notched antenna can effectively select target bands by adjusting these antenna parameters.

Finally, some conclusion and future works are drawn in Chapter 6.



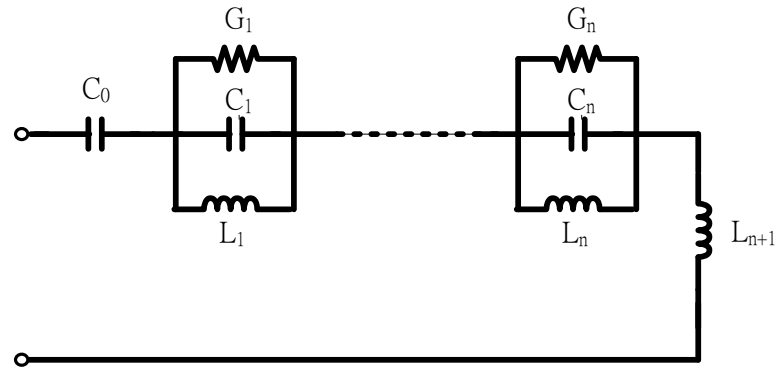
2 Fundamental theory and Architecture of Proposed Antenna



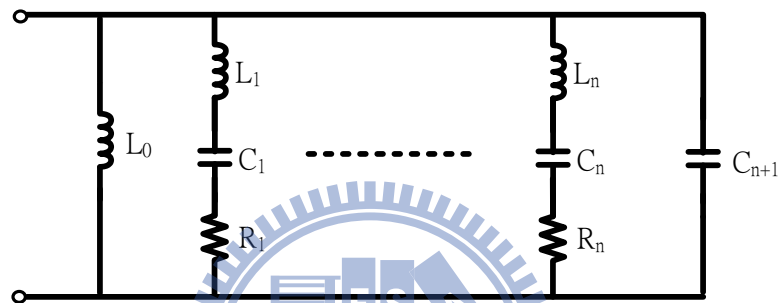
In chapter 2, the essential techniques to analyze the performance of UWB antenna are illustrated. Compared to the narrower band antenna design, these techniques are based on the conventional antenna measurement techniques and can describe the performance of UWB antenna over the extreme bandwidth. The Forster canonical forms for UWB antenna are described first. The system transfer function of a transmitting-receiving antenna system with identical antenna is consequently discussed. Through the transfer function measurement, the gain-frequency response and group delay are obtained. These techniques will be intensively used in the following sections. Finally, a notched-band UWB planar monopole antenna using the tapped-line coupled resonator is proposed and compared to the UWB antenna mentioned in the literature survey section.

2.1 Foster canonical forms and dimensionless normalized antenna transfer function for UWB antenna

Generally, an antenna is a linear and passive element whose input impedance can be represented by Foster canonical forms, as shown in Fig. 2.1, which assumes no ohmic loss [13]. Fig. 2.1 (a) is suitable for the modeling electric antenna like a dipole or monopole antenna, while Fig. 2.1 (b) is suitable for the modeling magnetic antenna like loop antenna. For UWB antenna, all the power radiated from the antenna is equal to the power dissipated on the resistors of Fig. 2.1. Fig. 2.1 can be employed to model the input impedance of UWB antenna when the impedance variation of RLC tanks is slow. In addition, according to Fig. 2.1, the UWB antenna can act as a wideband band-pass filter that introduces a frequency dependent response from the transmitter to the receiver. On the other hand, when the band-notched UWB antenna is considered, the behavior of Fig. 2 is a virtual transmission zero circuit or a band-stop filter. By shifting the input impedance of the antenna to a very high or very low level, the band-notched antenna restricts energy radiation or avoids interference.



(a)



(b)

Fig. 2.1 Forster canonical forms (a) electric antenna model (b) magnetic antenna model.

However, the circuit topology in Fig. 2.1 is insufficient to describe the radiated characteristics of UWB antenna because of the extremely large operating bandwidth. To tackle such a problem and to obtain the radiation characteristics of the UWB antenna, the dimensionless normalized antenna transfer function is used. Different from the general antenna transfer function, the dimensionless normalized antenna transfer function is the transfer function of an individual antenna and easily used in the antenna measurement. The detailed derivations are described as follows [21],[37],[38].

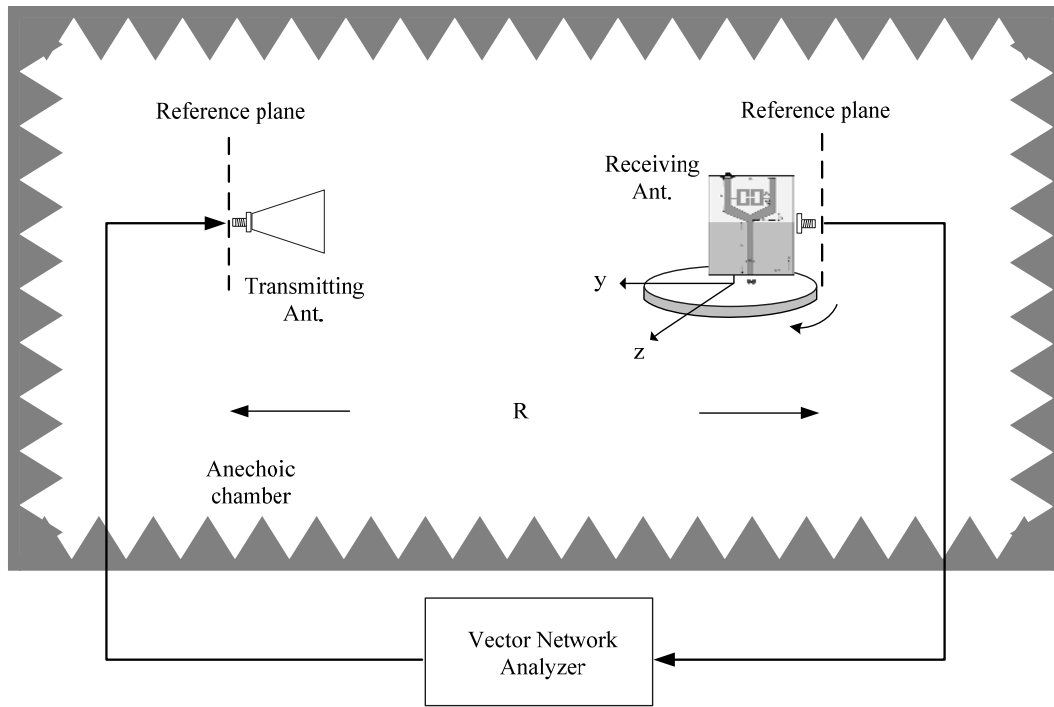


Fig. 2.2 Schematic diagram of the arrangement for measuring the system transfer function.

Referring to Fig 2.2, the antenna measured environment, the applied voltage $V_s(t)$ at the transmitting antenna terminal, the output voltage at receiving antenna terminal can be expressed by

$$V_{rec}(t) = \frac{1}{2\pi Rc} h_{N,Tx}(\tau, \theta, \phi) * \frac{d}{d\tau} V_s(\tau) * h_{N,Rx}(\tau, \theta, \phi) * \delta\left(\tau - \frac{R}{c}\right), \quad (2.1)$$

where $h_{N,Tx}(\tau, \theta, \phi)$ and $h_{N,Rx}(\tau, \theta, \phi)$ are the normalized impulse responses of the transmitting and receiving antenna, respectively. R is the distance between the antennas. The normalized impulse responses $h_{N,Tx}(t)$ and $h_{N,Rx}(t)$ in Equ.(2.2) are defined as

$$h_{N,Tx}(t) = \sqrt{\frac{Z_c}{Z_a}} \left(\frac{2Z_a}{Z_c + Z_a} * \sqrt{\frac{Z_\eta}{Z_a}} \right) h_{Tx}(t); \quad (2.2)$$

$$h_{N,Rx}(t) = \sqrt{\frac{Z_a}{Z_c}} \left(\frac{2Z_c}{Z_c + Z_a} * \sqrt{\frac{Z_\eta}{Z_a}} \right) h_{Rx}(t)$$

where $h_{Tx}(t)$ and $h_{Rx}(t)$ are the impulse response of the transmitting and receiving antenna, respectively. Z_c , Z_a and Z_η are the characteristic impedance of the measurement system, the antenna input impedance and the intrinsic impedance of free space. Equ.(2.1) is converted to frequency domain and accompanies with $S_{21}(f) = V_{rec}(f) / V_s(f)$. We get

$$\begin{aligned} S_{21}(f) &= \frac{j\omega}{2\pi RC} F \left\{ h_{N,Tx}(\tau, \theta, \phi) \right\} F \left\{ h_{N,Rx}(\tau, \theta, \phi) \right\} e^{-2\pi f \frac{R}{c}} \\ &= \frac{j\lambda}{4\pi R} H_{DN,Tx}(f, \theta, \phi) H_{DN,Rx}(f, \theta, \phi) e^{-2\pi f \frac{R}{c}} \end{aligned} \quad (2.3)$$

where

$$\begin{aligned} H_{DN,Tx}(f, \theta, \phi) &= \sqrt{\frac{4\pi}{\lambda}} F \left\{ h_{N,Tx}(t, \theta, \phi) \right\}; \\ H_{DN,Rx}(f, \theta, \phi) &= \sqrt{\frac{4\pi}{\lambda}} F \left\{ h_{N,Rx}(t, \theta, \phi) \right\} \end{aligned} \quad (2.4)$$

In Equ. (2.4), $H_{DN,Tx}(f, \theta, \phi)$ and $H_{DN,Rx}(f, \theta, \phi)$ are defined as dimensionless normalized antenna transfer function of transmitting and receiving antennas, respectively. $(4\pi / \lambda)^{0.5}$ is normalization factor.

According to Equ. (2.3), the conventional two-antenna gain measurement method can now be readily adopted to evaluate the antenna transfer function when the standard antenna

with constant group delay is well matched to the measured system. With this definition, the dimensionless normalized antenna transfer function of the antenna under test (AUT) can be determined

$$H_{DN,AUT}(f, \theta, \phi) = \frac{S_{21,AUT}(f, \theta, \phi)}{S_{21,STD}(f)} H_{DN,STD}(f) \quad (2.5)$$

where $S_{21,AUT}(f, \theta, \phi)$ is the measured transmission scattering parameter of AUT at a specific angle (θ, ϕ) . $S_{21,STD}(f)$ is that of the standard antenna in its maximum gain direction, and $H_{DN,STD}(f)$ is the dimensionless normalized antenna transfer function of the reference standard antenna which is given by

$$H_{DN,STD}(f) = \sqrt{G_{STD}(f)} \cdot e^{j2\pi f \cdot t_d} \quad (2.6)$$

where $G_{STD}(f)$ and t_d are the absolute gain and group delay of standard antenna, respectively.

By substituting Equ.(2.6) to Equ.(2.5), the normalized antenna transfer function of AUT can be readily achieved.

In our measurement, the EMCO 3115 double-ridge horn antenna is used as the standard antenna. This antenna with a constant group delay of 630ps is well matched to the measuring system. The distance between the standard antenna and the proposed antenna was 3.6m. Following the measurement procedure, the time gating technique of vector network analysis is applied during measurement to reduce effect of rich multi-reflection interference, meanwhile, the narrower IF bandwidth is adopted to increase signal to noise ratio (SNR). With these two

measurement skills, the accuracy of group delay and gain response can be significantly improved by setting the time gating window and IF bandwidth as 3ns and 700Hz, respectively.

2.2 A Band-Notched UWB Planar Monopole Antenna with Tapped-Line Coupled Resonator

In this subchapter, a band-notched UWB antenna planar monopole antenna with tapped-line coupled resonator is presented. The proposed antenna has shown band-notched performance due to the proper-positioned tapped-line coupled resonator at the fork-shaped antenna. The length and the feeding position of resonator are also discussed in this work. The proposed antenna also features flat gain frequency response, slightly varied group delay and 10 to 18dB gain suppression in the notch band.

2.2.1 Geometry and design concept

Figure 2.3 shows our proposed notched band monopole antenna. The antenna consists of a forked-shaped radiator and a tapped-line coupled resonator. The fork-shaped antenna is designed for the wide operating range and the resonator is placed at the antenna center. By this arrangement, the effects of the resonator can be emphasized. The antenna was fabricated

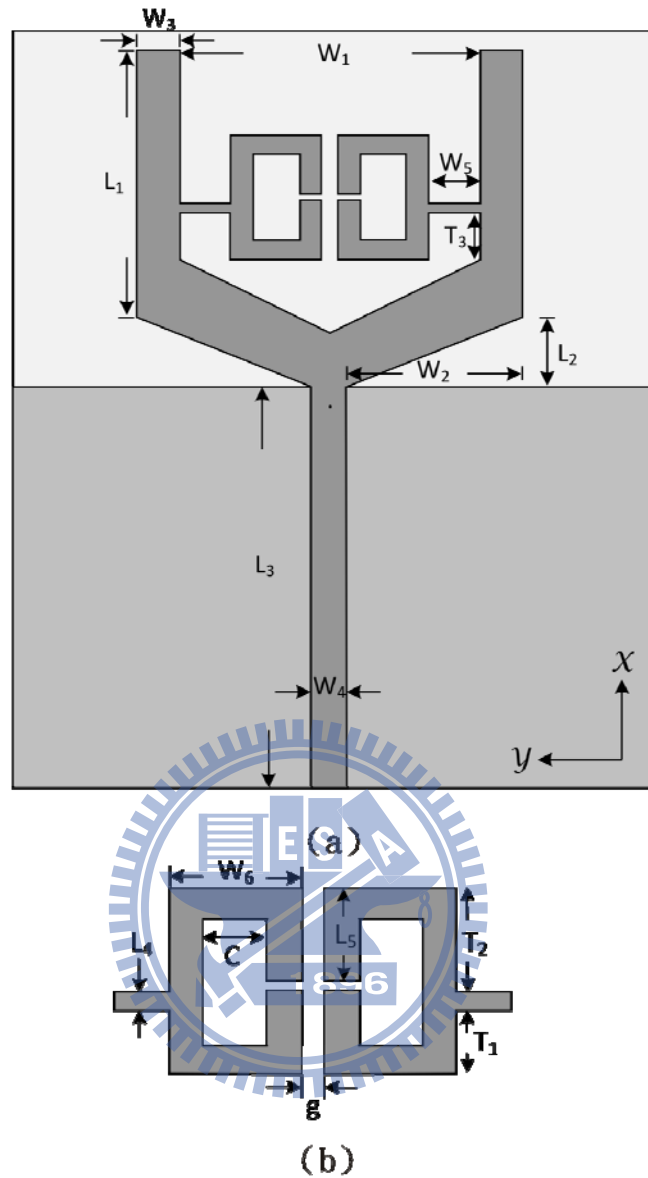


Fig. 2.3 Configuration of the proposed antenna. (a) Top view. (b)The proposed resonator.

on a 0.77mm RO4350 substrate with overall size of 36mm by 30mm. The final antenna parameters are optimized and are given as follows: $W_1=14, W_2=8.15, W_3=2, W_4=1.65, W_5=2.4, W_6=4.2, L_1=12.7, L_2=3.3, L_3=19, L_4=0.4, L_5=2.8, T_1=2.3, T_2=3.3, T_3=3.3, C=2.2, g=0.8$, where all units are in mm.

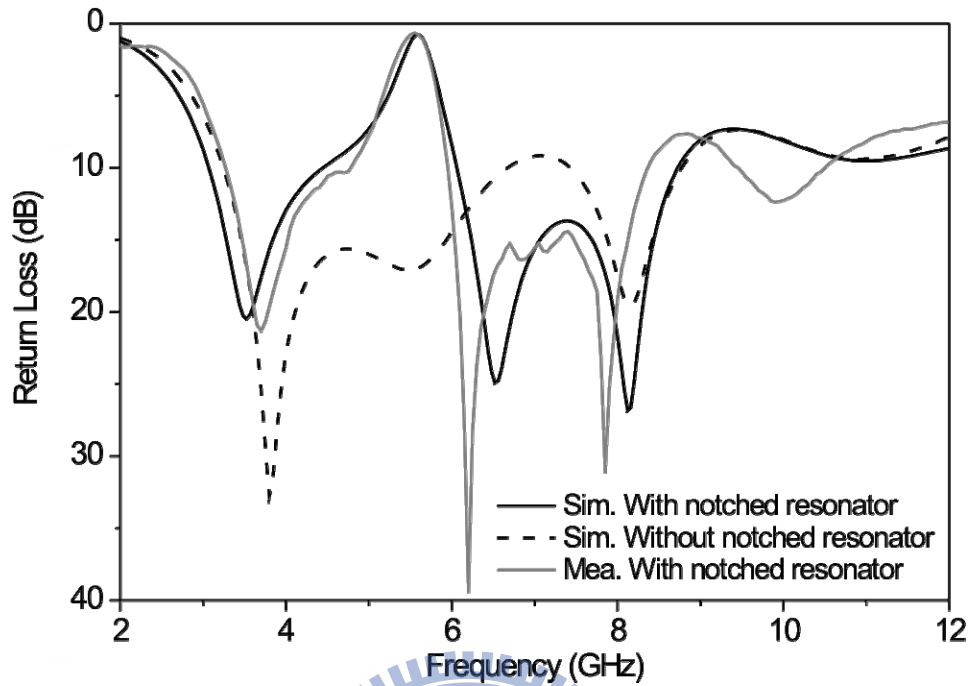


Fig. 2.4 Simulated and measured return loss of the proposed antenna.

The simulated and measured return losses of the proposed antenna are show in Fig. 2.4.

Ansoft HFSS 9.2 is used in the simulation while the measurement uses an Agilent E8362B performance network analyzer. The agreement between the simulation and measurement is fairly good over the operating band. The measured notched bandwidth is from 4.75 to 5.95 GHz with 0.67 dB return loss level at the notched band center. It is also evident that the proposed resonator only slightly interferes with the return loss of the fork-shaped antenna, except within the notched band.

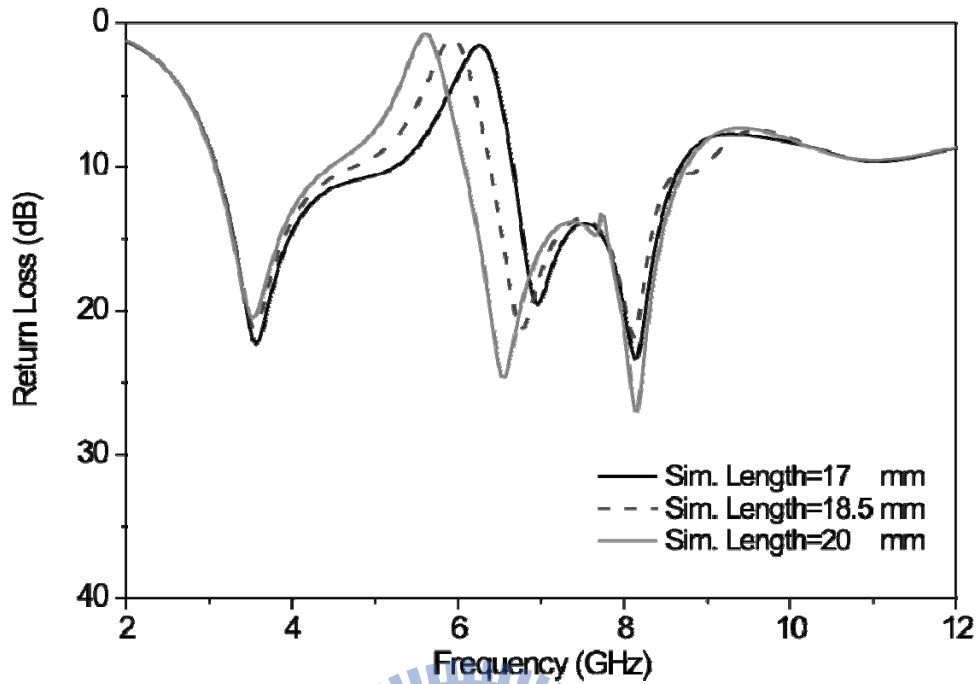


Fig. 2.5 Simulated return loss at various lengths of the resonator.

2.2.2 Design guideline and performance

The most importance parameters of band-notched effect, i.e., the electric length and the feeding position of the resonator are shown in Fig. 2.5 and Fig. 2.6 respectively. Fig. 2.5 shows the simulated return loss at various lengths of the resonator. To obtain the different resonance frequency, the resonator remains original shape and changes the electrical length. The center notched frequency varies from 5.6 GHz to 6.28 GHz as the electrical length of the resonator changes from 8 mm to 6 mm. The center frequency of the notched band is simply inversely proportioned to the resonator length.

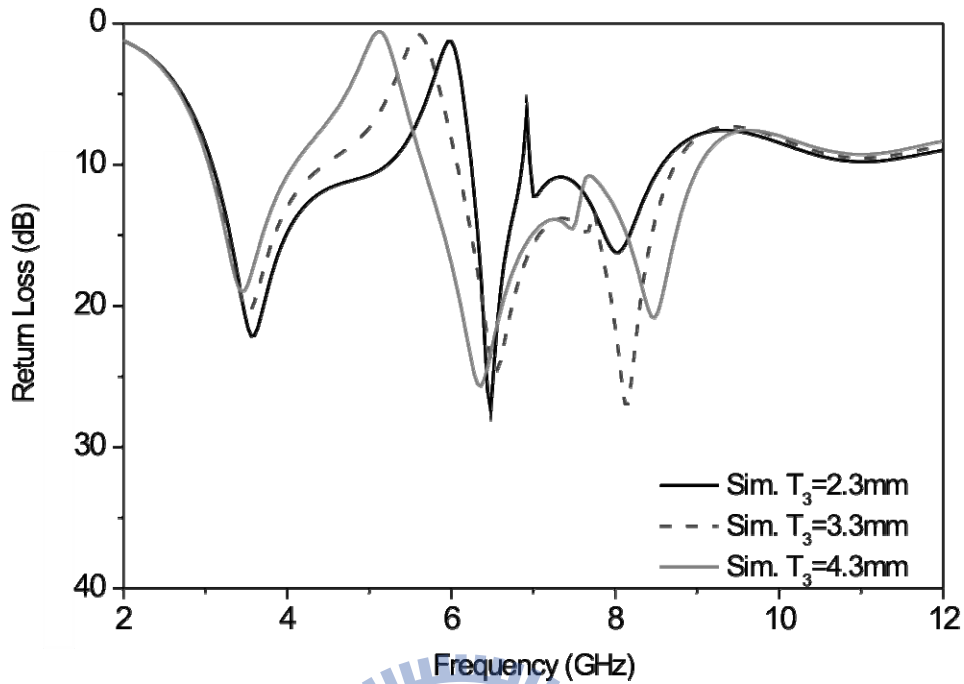


Fig. 2.6 Simulated return loss at the various feeding locations of resonator at antenna.

Figure 2.6 shows the simulated return loss at various feeding locations of the resonator.

It is found that the center notched frequency varies from 5.12 GHz to 5.96 GHz as T_3 changes from 4.3 mm to 2.3 mm at the fixed T_1 and T_2 . The notched frequency dramatically varied due to the variation of the resonant and the quality factor of the resonator. It should be noted that different from the general resonator design concept, which is the location of feeding line at resonator cannot be a dominant factor on the resonant frequency, the notched frequency of antenna is strongly related to the feed position of the resonator in this work.

The proposed antenna radiation patterns are measured in a $7.0 \times 3.6 \times 3.0 \text{ m}^3$ anechoic chamber with an Agilent E362B network analyzer along with the NSI2000 far-field

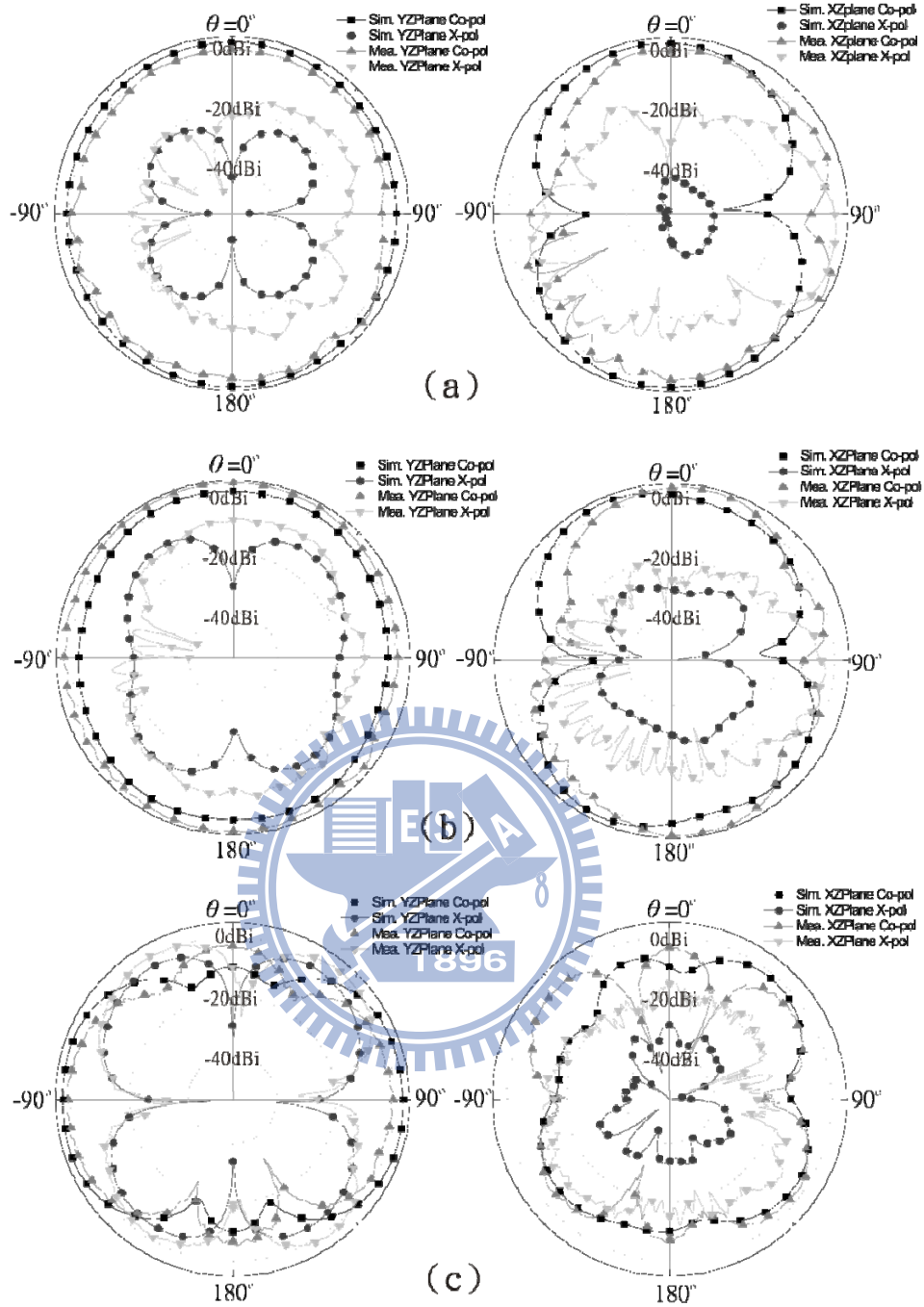


Fig. 2.7 Measured and Simulated radiation patterns at (a) 4GHz. (b) 7GHz. (c) 10GHz. (Unit:dBi)

measurement software. The H- (yz-) and the E- (xz-) plane radiations at 4GHz, 7GHz and 10GHz are shown in Fig. 2.7. It can be seen that the patterns of proposed antenna present

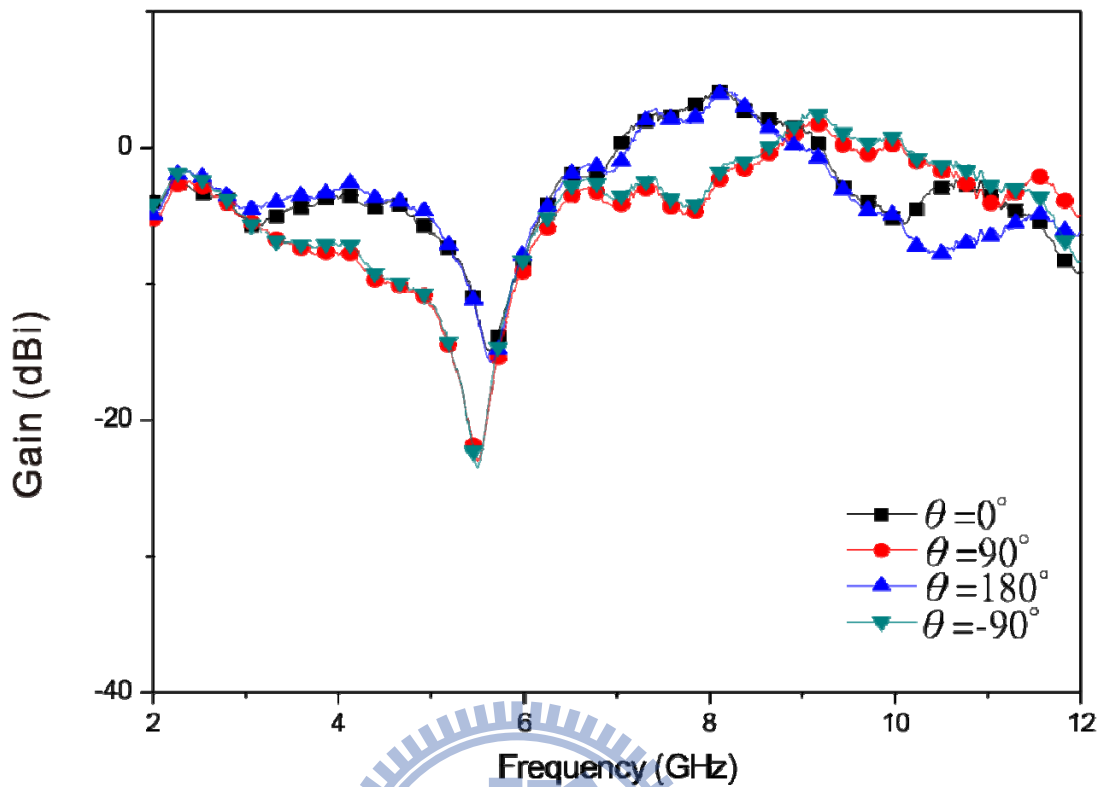


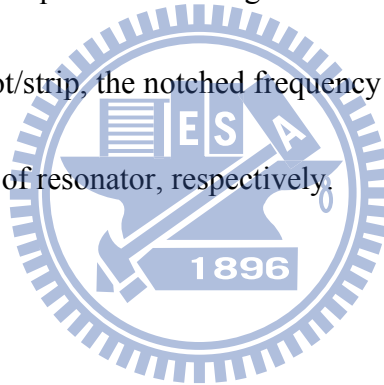
Fig. 2.8. Measured gain response of the proposed antenna. at $\theta=0^\circ$, $\theta=90^\circ$, $\theta=180^\circ$, $\theta=-90^\circ$.

nearly omni-directional and stable radiation characteristic in yz-plane whereas it becomes similar to a roughly dumbbell like shape over the frequency band in the xz-plane. The cross-polarization levels are generally much lower than co-polarization ones.

Fig. 2.8 illustrates the measured gain responses in yz-plane at four specific angles, i.e., from -180° to 180° with 90° step. As shown in Fig. 2.8, the gain responses of proposed antenna are quite stable over the frequency of interest. At target notched band, the band-notched phenomenon can be readily observed and the gain suppression at least 10dB

and as high as 18dB.

In order to compare proposed antenna to other band-notched antennas, Table 2.1 shows six miniature band-notched UWB antenna structures in [6]-[8], [23], [27] and [32]. In general, each notched band of these antennas is achieved by cutting the thin slit, adding the plastic strip or placing the resonator. The plastic strip/slot and the part of antenna form a resonant structure which leads to a sudden change in the impedance in the notching frequency. These lengths usually proportion to a half wavelength of notched frequency for both the short-end slit and open-end strip or a quarter wavelength of notched frequency for open-end slit. Different from the plastic slot/strip, the notched frequency is mostly depended on the resonant frequency and quality factor of resonator, respectively.



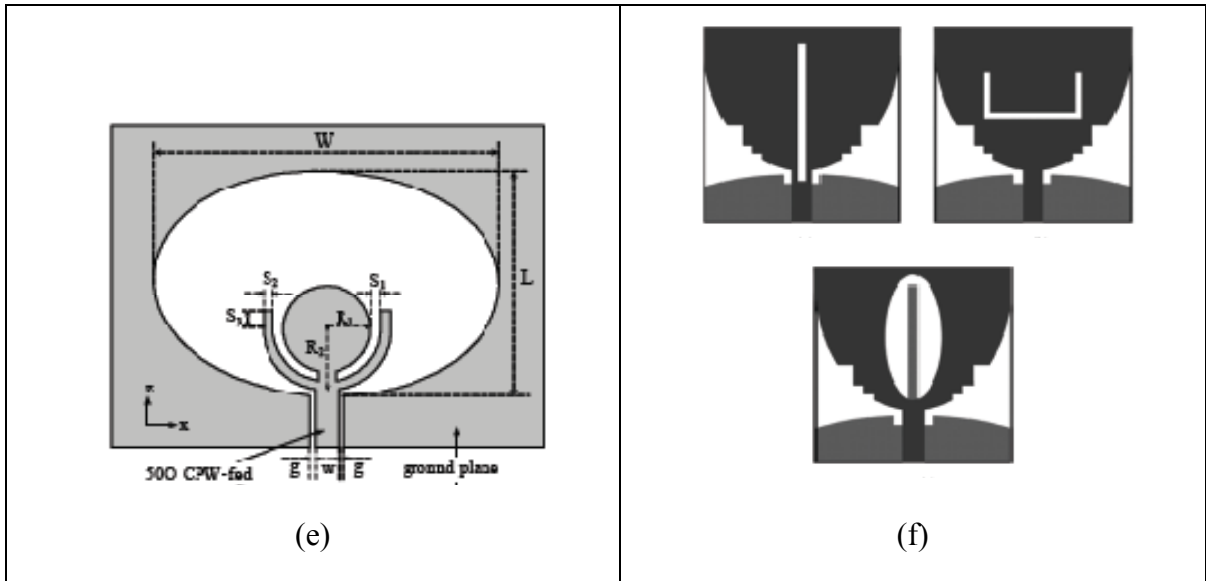


Table 2.2

The compared results of the band-notched antennas

	Antenna size (Unit: mm ²)	Maximum suppression (Unit: dB)	Gain	Notched bandwidth (Unit : GHz and on 10dB RL condition)
Proposed antenna	18 x 32 = 576	18		4.75-5.95
Table 2.1 (a)	24 x 35 = 840	~10		5-6
Table 2.1 (b)	22 x 22 = 484	~10		5-6
Table 2.1 (c)	25 x 26 = 650	~8		5-5.8
Table 2.1 (d)	35 x 30 = 700	~8		5-6
Table 2.1 (e)	30 x 25 = 750	~8		5-6
Table 2.1 (f)	20 x 20 = 400	~6		5-6

The compared result is illustrated in Table 2.2. According to Table 2.2, the proposed antenna has compact size and good gain suppression in the notched band. These features of the proposed antenna demonstrate that the proposed antenna is suitable for UWB communicational applications and prevents interference from the WLAN system.

2.3 Summary

The impedance of UWB antenna with/without resonator has been described by the Forster canonical forms. The UWB antenna can be represented as the wideband band-pass filter that introduces a frequency dependent response from the transmitter to the receiver. On the other hand, the band-notched UWB antenna is a virtual transmission zero circuit or a band-stop filter in the notched band. The detailed derivations of dimensionless normalized antenna transfer function are discussed consequently. Different from the general antenna transfer function, the dimensionless normalized antenna transfer function is a transfer function of an individual antenna and easily used in the antenna measurement. To measure the gain-frequency response and group delay, the measurement procedures as well as arrangements are introduced. Finally, the band-notched UWB antenna planar monopole antenna with tapped-line coupled resonator had been presented. The proposed antenna has shown band-notched performance due to the proper-positioned tapped-line coupled resonator at the fork-shaped antenna. The proposed antenna also features flat gain frequency response

and 10 to 18dB gain suppression in the notched band. These features of the proposed antenna demonstrate that the proposed antenna is suitable for UWB communicational applications and prevents interference from the WLAN system.

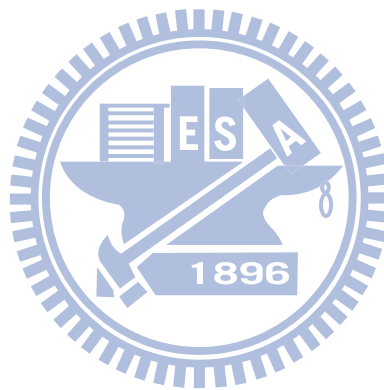


3 Planar Band-Notched UltraWideband Antenna with Square-Looped or End-Coupled Resonator



A square-looped or an end-coupled resonator used in a planar ultra-wideband (UWB) antenna to achieve the band-notched performance are presented. To obtain the notched performance in WLAN band, both the square-looped and end-coupled resonator are designed and placed in the fork-shaped UWB antenna center. The characteristics and schematic equivalent circuit of each resonator are discussed. The parametric studies of fork-shaped antenna with square-looped resonator are treated as an example to explore the operating mechanism. Accordingly, the band-notched antenna can effectively select target bands by adjusting different resonator structures. The proposed antenna features flat gain frequency response, small varied group delay and 10 to 25 dB gain suppression in the notched band.

In section 3.2, the fork-shaped UWB antenna with the square-looped resonator or end-coupled resonator is consequently presented. The geometry and design concept of each resonator is presented and discussed. The comparison between square-looped resonator and the tapped-line coupled resonator in section 2.3 is further discussed. In section 3.3, the parameters studies of the proposed antenna with square-looped resonator explain the basic resonant behaviors. Consequently, the gain-frequency transfer function and group delay are presented. Finally, Section 3.4 provides our conclusion.



3.1 Geometry and Design Guideline

3.1.1 Geometry of the proposed antenna

Figure 3.1 shows the geometry of the proposed antenna, consisting of the fork-shaped UWB antenna and the square-looped resonator. The fork-shaped UWB antenna design is based on a triangular-shaped radiator and U-shaped radiator in [13],[14]. The bevel profile of fork-shaped UWB antenna, section of W_2 and L_2 , enhances the wide operating bandwidth especially for higher frequency because it is slow down the impedance variation from microstrip line to free space. Meanwhile, the lowest frequency is determined by the length of $L_1+L_2+W_2$. Furthermore, the majority of the electric currents are concentrated around the narrow portion of the fork-shaped UWB antenna. Hence, the resonator position at the interior of the antenna not only determines the band-notched characteristics, but also nearly remains the original essential characteristics of the antenna. The inner cutting triangular area, 0.5×2.5 mm x 14 mm, is applied here to place the proposed resonators.

The simulated software, Ansoft HFSS 9.2, is used while the measured equipment is adjusted by an Agilent E8362B performance network analyzer. The antenna was fabricated on a 35 mm x 30 mm x 0.77 mm Rogers RO4003 substrate with dielectric constant $\epsilon_r = 3.28$ and loss tangent = 0.004 at 10 GHz. The final design parameters are $W_1 = 14$, $W_2 = 8.3$, $W_3 = 2$, $W_4 = 1.4$, $W_5 = 1.8$, $W_6 = 0.8$, $W_7 = 5$, $L_1 = 13$, $L_2 = 2.5$, $L_3 = 20$, $L_4 = 2.5$, $L_5 = 0.4$, $L_6 = 2.8$, $L_7 = 2.8$, $L_8 = 6$, $g = 0.4$ where unit is mm.

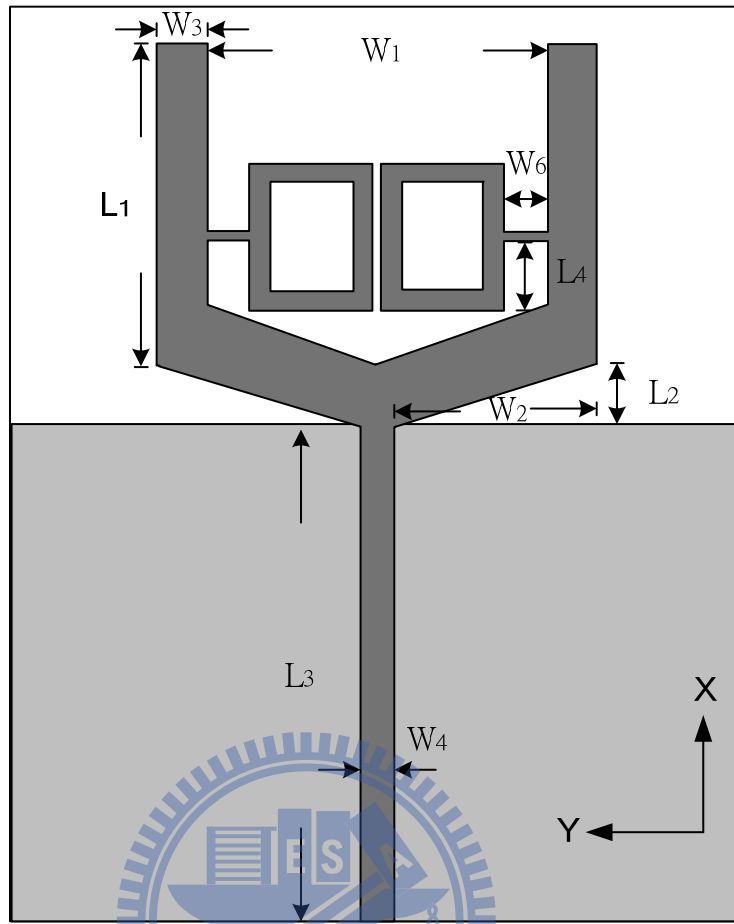


Fig. 3.1. Geometry of proposed antenna.

Figure 3.2 shows the simulated and measured VSWR. It demonstrates the resonant behavior, which leads to the desired impedance mismatching near the notched frequency at 5.6GHz. The measured result agrees with the simulated one and determines that only slightly interferes the operating bandwidth of the fork-shaped UWB antenna except within the notched band. The notched band reveals the narrow bandwidth and the fast roll-off rate due to the high quality factor and the appropriate position of the resonator.

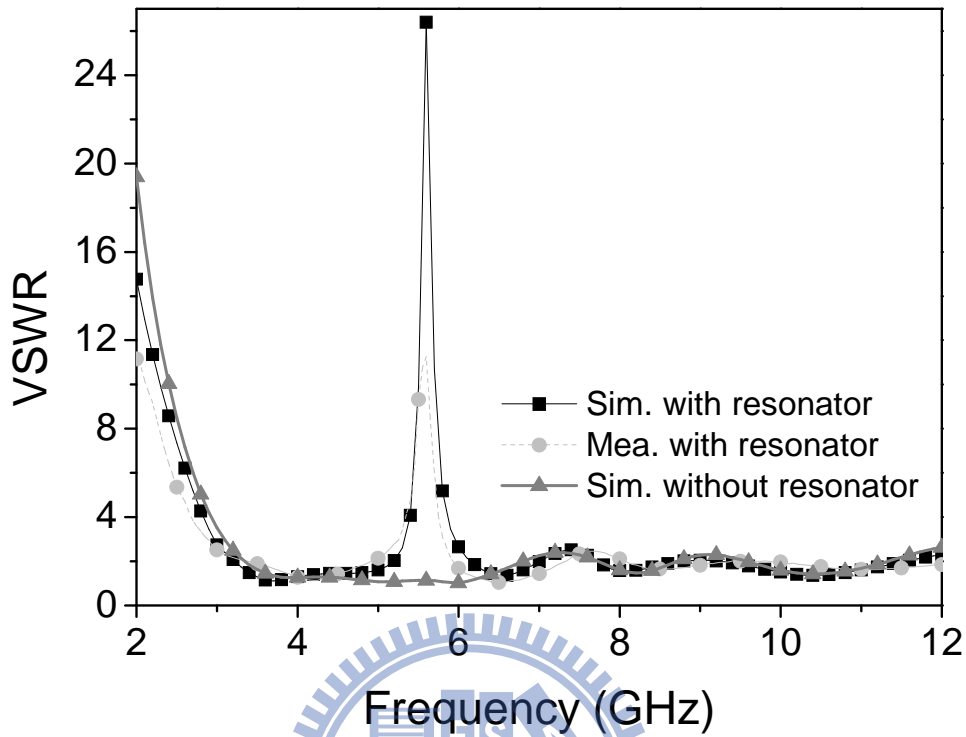


Fig. 3.2. Measured and simulated VSWR of fork-shaped UWB antenna with square-looped resonator.

3.1.2 Square-looped resonator and End-coupled resonator

Figs. 3.3(a) and (b) show the square-looped resonator and tapped-line coupled resonator of [22], respectively. The short strip, W_5 , connects the proposed resonator and the fork-shaped UWB antenna. Basically, Fig. 3.3 (a) and (b) have similar geometry model. The difference between them is the gap of s . Hence, the Fig. 3.3(a) can be treated as a half wavelength ring resonator while Fig. 3.3(b) is an open-ended resonator which shuts a pair of quarter wavelength strip. There are two observations are worthwhile when the fork-shaped UWB

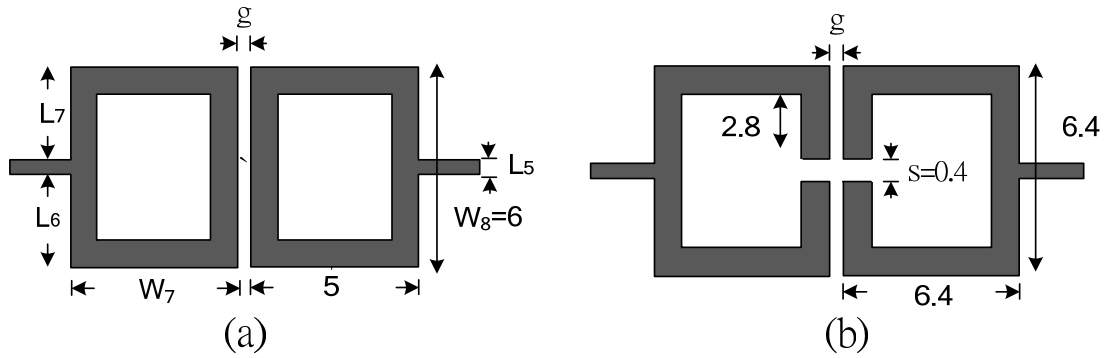


Fig. 3.3 (a) Square-looped resonator structure; (b) Tapped-line coupled resonator

antenna uses a resonator of Fig. 3.3(b). One is the fringe field at open-end of resonator is decrease because the resonator is floating. Another is when the resonator has a different length of each strip, the antenna may have two notched frequencies.

The square-looped resonator can be represented by the lossless parallel tuned-circuit as shown in Fig. 3.4. The mutual coupling, C_m , is determined by the gap of g . The notched frequency is mainly determined by the resonance of each sub-loop (L_{eq} and C_{eq}) and the gap of g (C_m). Through the simulation, the gap of g slightly effects the resonant frequency even if it varies from 0.2 to 1.4mm. Thus, for notched frequency controllability, the variation of mutual coupling is not a key factor but the length is domination.

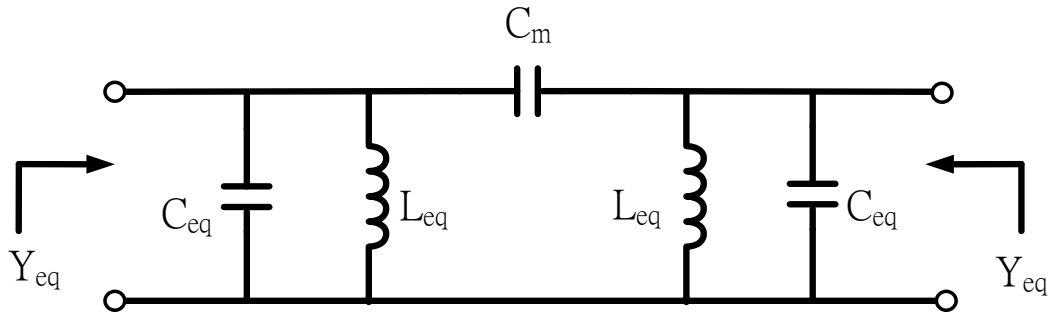


Fig. 3.4 Schematic equivalent circuit of square-looped resonator.

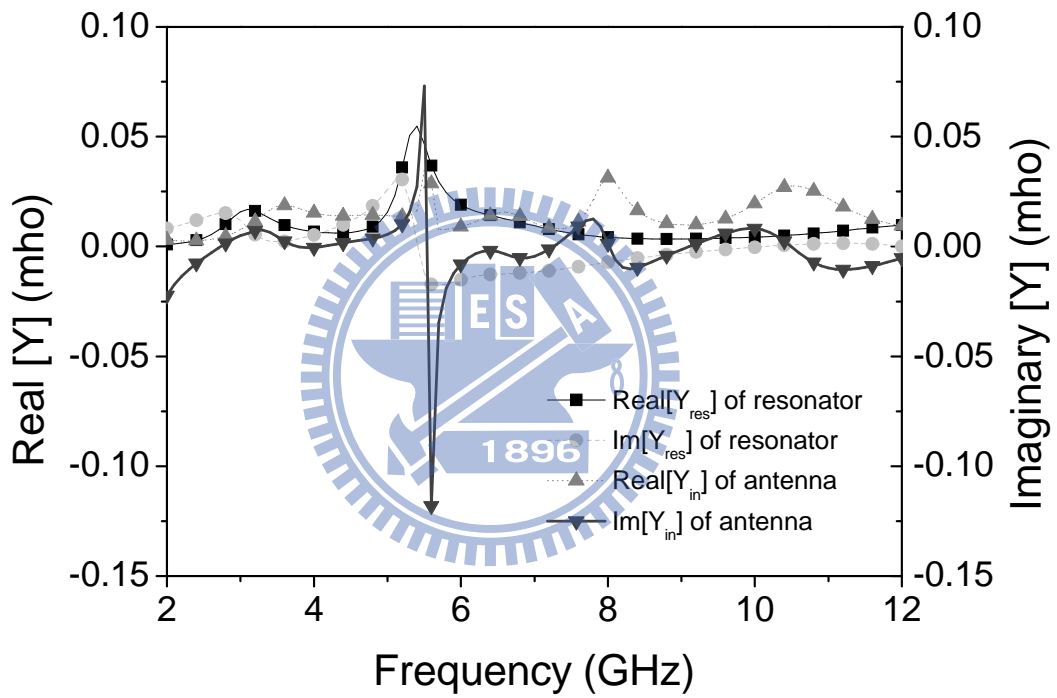


Fig. 3.5 Admittances of the proposed antenna.

Figure 3.5 shows the simulated admittances of the proposed antenna as shown in Fig.3.1 and square-looped resonator itself, respectively. The resonant frequency of square-looped resonator is quite similar with the notched frequency of the proposed antenna.

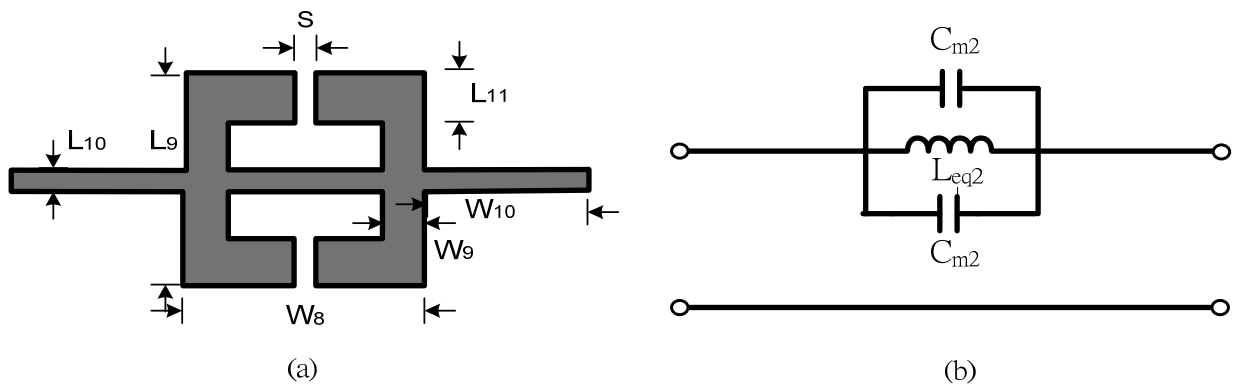


Fig. 3.6 (a) End-coupled resonator structure (b) Schematic equivalent circuit of end-coupled resonator.

It demonstrates the parallel resonant behavior, which leads to the desired impedance mismatching at 5.6GHz.

Figs.3 6(a) and (b) illustrate a proposed end-coupled resonator and its schematic equivalent circuit, respectively. The end-coupled resonator has compact size, $4.4 \times 4.4 \text{ mm}^2$ only, and is composed of a strip line with a pair of folded open stubs which forms the coupled loads, C_{m2} , as shown in Fig. 3.6(b). In this case, the resonant frequency of resonator is determined by the length of folded open stubs and coupled loads.

Figure 3.7 shows the simulated and measured VSWR of the fork-shaped UWB antenna with end-coupled resonator. The parameters of end-coupled are followed: $W_8 = 4.4$, $W_9 = 0.8$, $W_{10} = 5.8$, $L_9 = 4.4$, $L_{10} = 0.4$, $L_{11} = 1.0$ and $S = 0.4$ where the unit is mm. As shown in Fig. 3.7, the measured result agrees with the simulated one. The impedance of end-coupled resonator is quite similar than square-looped resonator and does not show here for simplification.

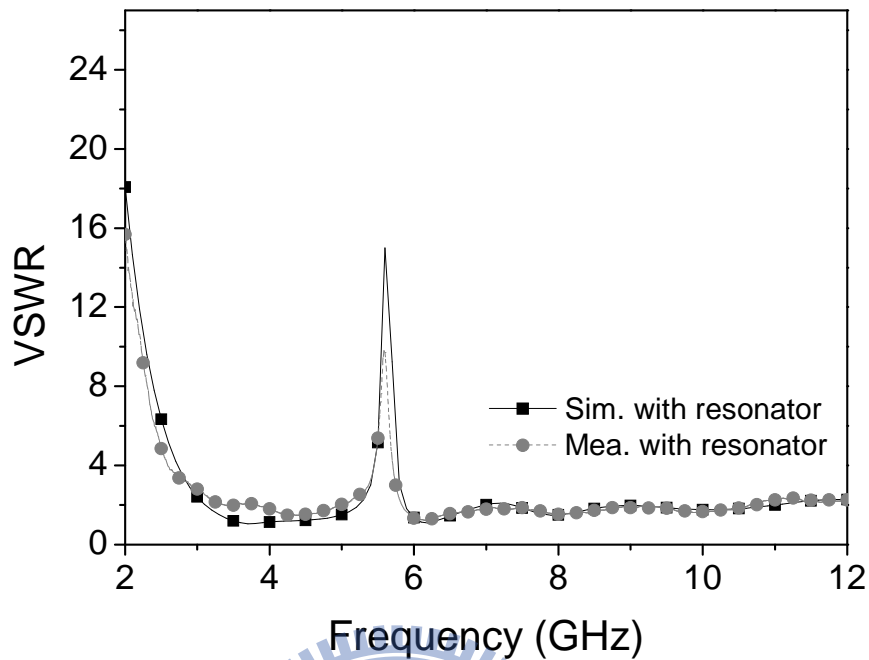
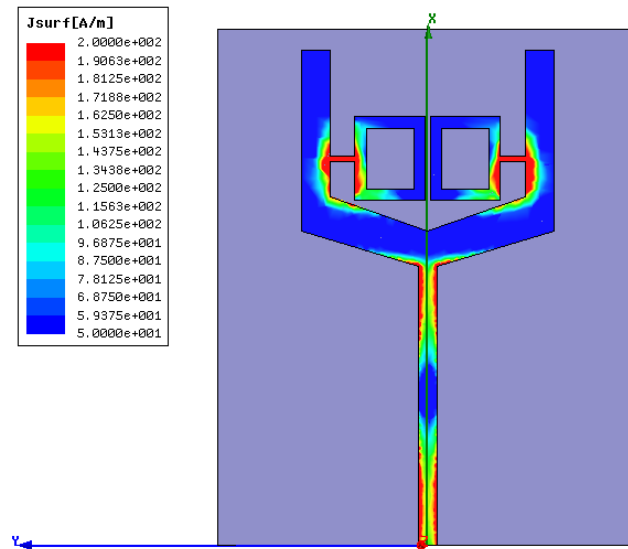


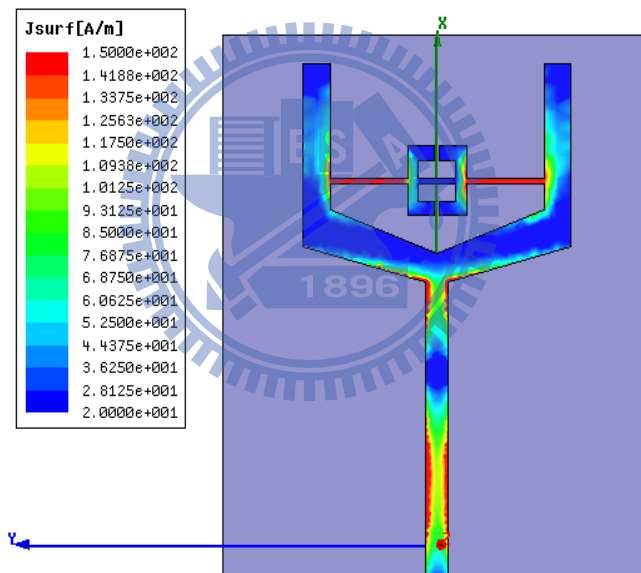
Fig. 3.7 Measured and simulated VSWR of the fork-shaped UWB antenna with end-coupled resonator.

3.2 The performance of fork-shaped UWB antenna with square-looped resonator

Because the performance of both the square-looped resonator and end-coupled resonator are similar, the square-looped resonator are chosen in the following discussions for simplification. Hence, in the following subsections, the geometric parameters of the square-looped resonator based on its length, feeding position, and position are firstly investigated. The measured patterns and gain response versus frequency at 8 angles as well as group delay are following presented.



(a)



(b)

Fig. 3.8 Simulated current distribution of the proposed antenna at 5.5 GHz.(a) square-looped resonator. (b) end-coupled resonator.

The simulated current distribution at 5.8 GHz is shown in Fig. 3.8. It reveals that the currents mainly concentrate over the area of the proposed resonators in the radiation patch.

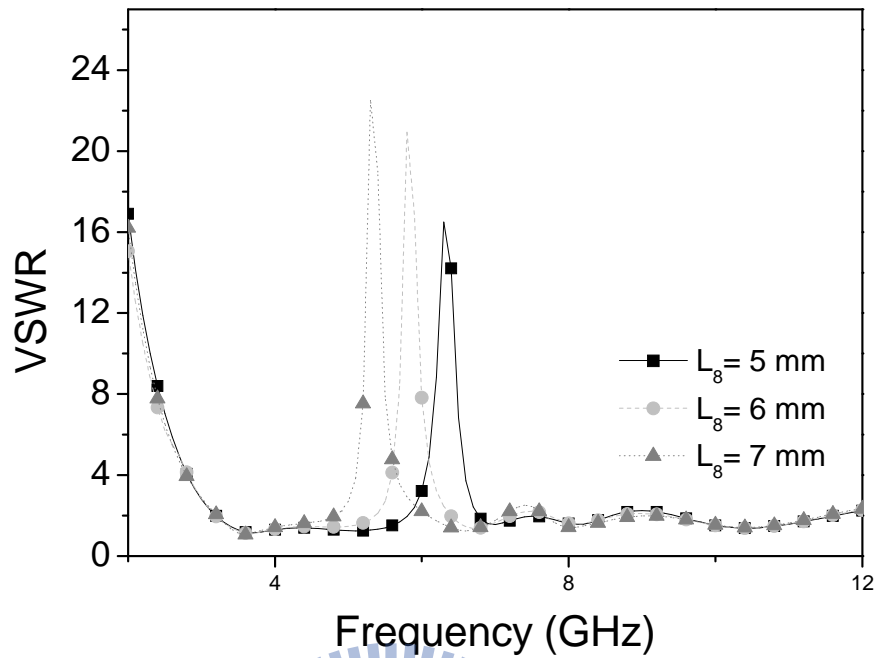


Fig. 3.9 VSWR versus the various lengths of the square-looped resonator.

3.2.1 Parametric Study

Figure 3.9 exhibits VSWR versus the various lengths of the square-looped resonator. It is clearly seen that the length of the square-looped resonator has significant effect on the notched frequency. The notched frequency shifts from around 5.2 GHz to 6.3 GHz as the length of square loop changes from 20 to 24mm. (L_8 changes from 5 to 7 mm). This is due to the resonant frequency of square-looped resonator is simply in reverse proportion to the length of the resonator.

Figure 3.10 exhibits VSWR versus the various input positions of the square-looped resonator. In this case, only the strip, W_5 , moves in x-oriented. The location

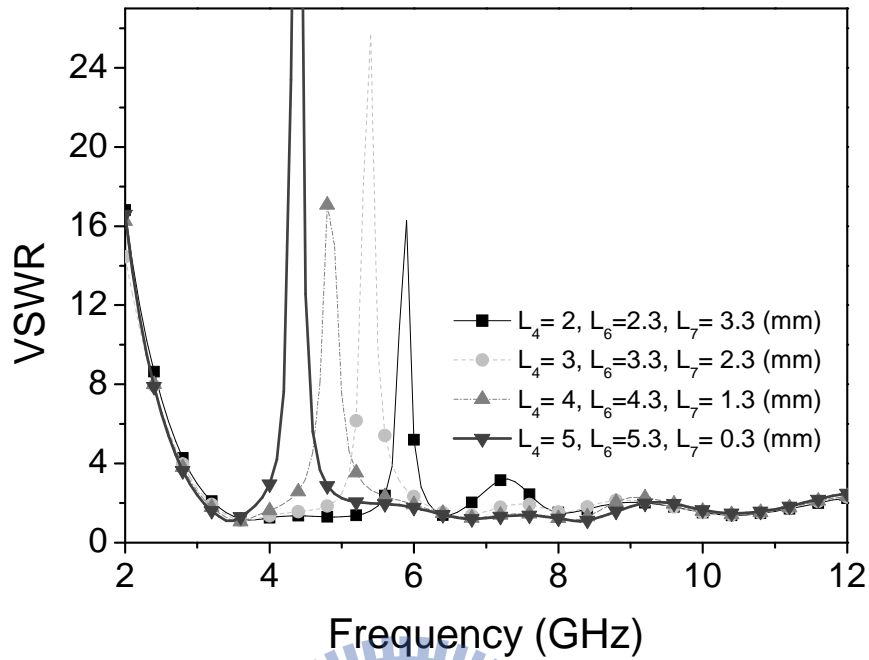


Fig. 3.10 VSWR versus the various input positions of the square-looped resonator.

of the short strip in the x-oriented has significant effect on the notched frequency. Compared with the resonant frequency variation of both the resonator and proposed antenna in the same condition, the variation of proposed antenna is significantly bigger than one of resonator. It is implied that the part of fork-shaped UWB antenna, from the microstrip line to the input position of resonator, effect the notched frequency because the extra inductance property is added into the resonator. In my opinion, when a resonator is treated as the part of radiator, the path from signal source to resonator can be modeled as an extra circuit network which affects the notched frequency and external quality factor of whole antenna in the notched band.

Figure 3.11 exhibits VSWR versus the various positions of the resonator in the

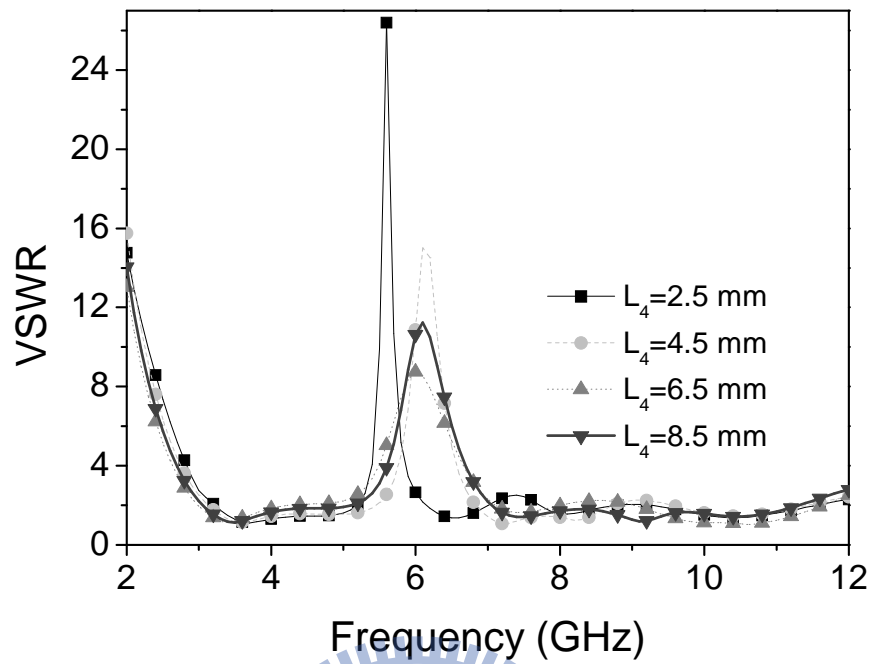


Fig. 3.11 VSWR versus the various positions of the resonator in the x-oriented.

x-oriented, i.e., various values of L_4 while resonator structure is fixed. In this case, whole resonator moves together. The center frequency of the notched band is small change, whereas bandwidth of the notched band is significantly larger as the resonator is placed at the near end of the fork-shaped UWB antenna. It implies that when the resonator is placed near the end of the fork-shaped antenna, the external quality factor becomes lower and the bandwidth of the notched band becomes wider simultaneously.

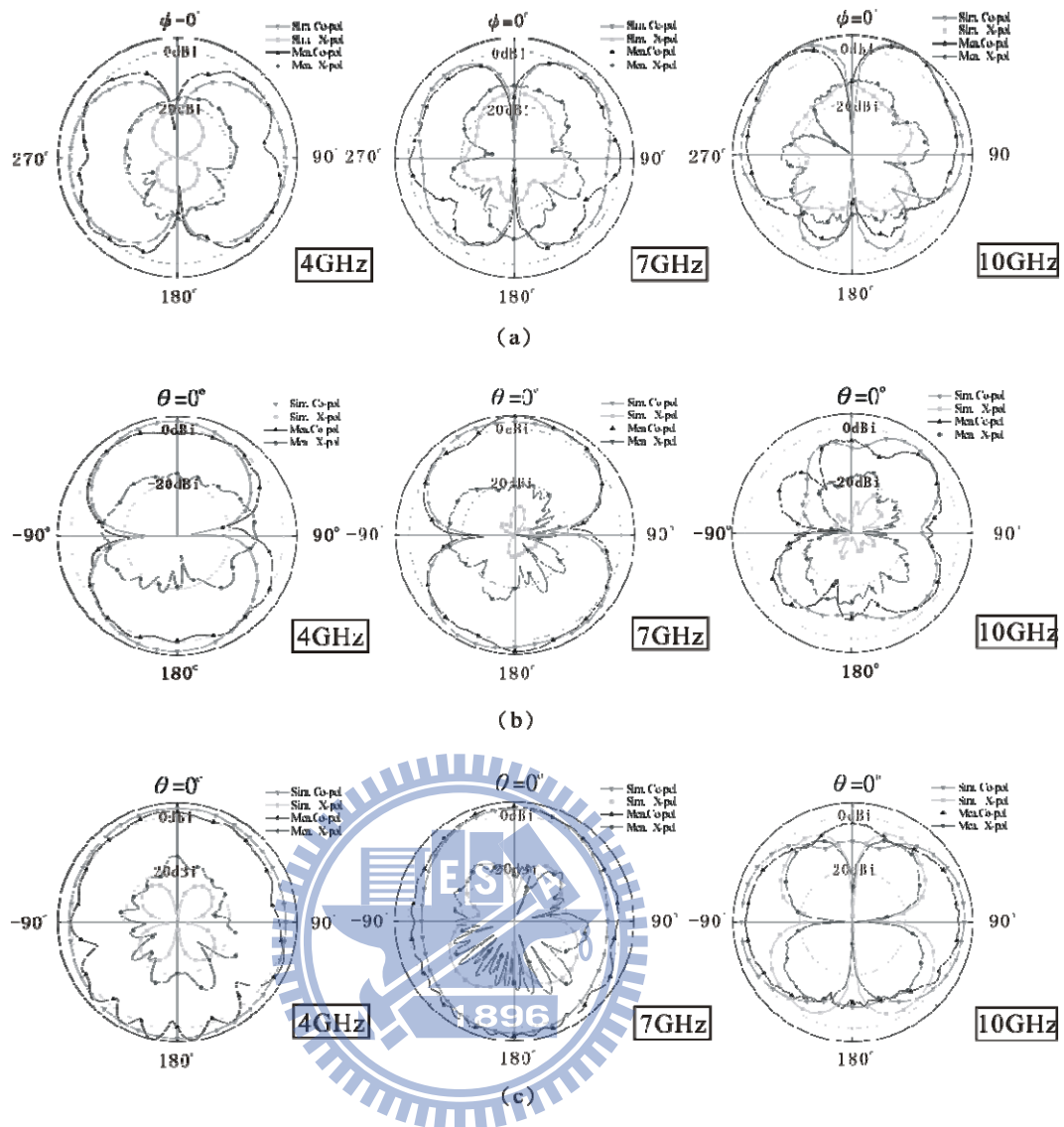
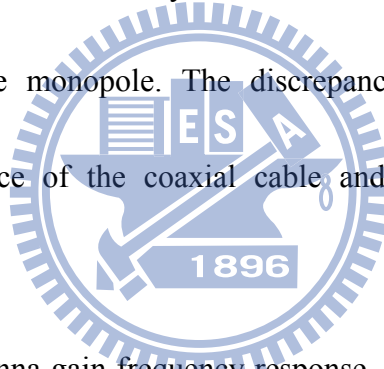


Fig. 3.12 Measured and Simulated radiation patterns at (a) xy-plane. (b) xz-plane. (c) yz-plane. (Unit:dBi)

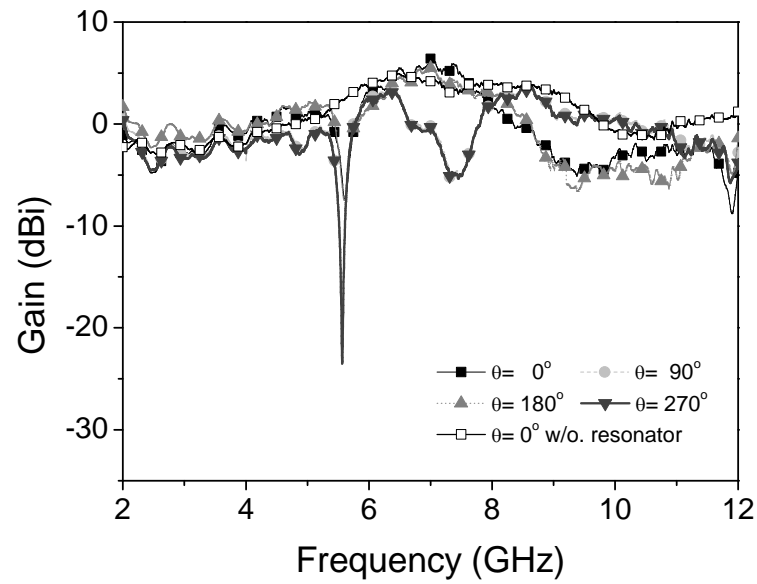
3.2.2 Radiation Patterns, Gain response and Group Delay

The antenna radiation patterns, gain response and group delay are measured in a 7.0 x 3.6 x 3.0 m³ anechoic chamber with an Agilent E8362B network analyzer along with NSI2000 far-field measurement software.

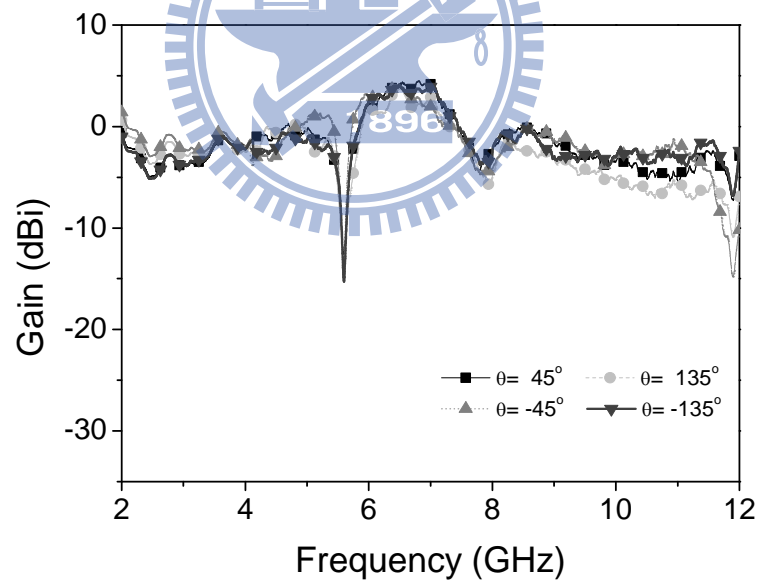
Figure 3.12 shows the measured and simulated radiation patterns in the xy -, xz -, and yz -planes at 4, 7, and 10 GHz. The measured patterns agree with the simulated ones. Referring to Figs. 3.12(a) and (b), the co-polarization patterns are roughly dumbbell-like shapes and the cross-polarization levels are much lower than co-polarization levels. In Fig. 3.12(c), the co-polarization patterns have a probably omni-directional shapes at lower frequency and dumbbell-like shapes at higher frequency. The cross-polarization level rises considerably as frequency increases because the resonator directly integrated into antenna layout produces the substantial level of y -oriented radiation in addition to main x -oriented radiation field of fork-type monopole. The discrepancies of cross-polarizations can be attributed to the interference of the coaxial cable and the absorbers used in measured arrangement.



In the measuring antenna gain frequency response, the EMCO 3115 double-ridge horn antenna with a constant group delay of 680 ps is used as a reference antenna for calibration. Figure 3.13 illustrates the measured gain frequency responses in the yz -plane at eight angles, ranged from -180° to 180° with 45° interval. According to Fig.12, the range of gain suppression is from 10 dB to 25 dB for these eight angles at the target notched band. The notched frequencies are quite similar at the observation angles. The notched bandwidth is significantly narrower due to the fast roll-off rate and high quality factor of proposed resonator.



(a)



(b)

Fig. 3.13 Measured gain response (a) $\theta = 0^\circ$, $\theta = 90^\circ$, $\theta = 180^\circ$, $\theta = 270^\circ$. (b) $\theta = 45^\circ$, $\theta = 135^\circ$, $\theta = -45^\circ$, $\theta = -135^\circ$.

Figure 3.14 presents the measured group delay of the proposed antenna. Except the

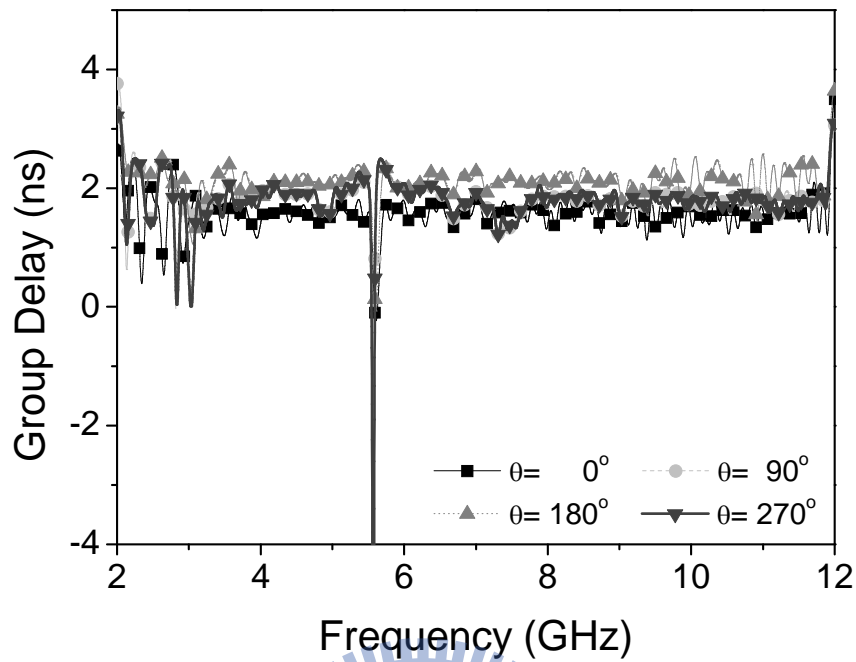


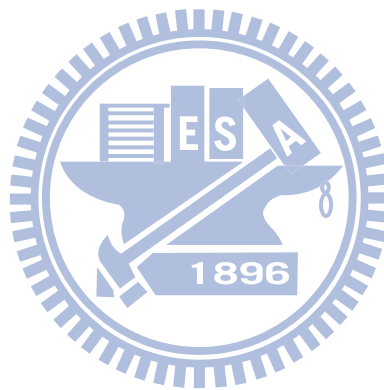
Fig. 3.14 Measured group delays.

notched band, the variation of group delay variation over the 3.1 to 10.6 GHz is less than 860 ps with its average of 1.6 ns as the spatial angle varies. In the notched band, the impedance mismatch between the proposed antenna and far-field measurement system causes the inaccurate and negative group delay. Figures 3.13 and 3.14 show that the proposed antenna has good time/frequency characteristics and a small pulse distortion over the UWB operated band.

3.1 Summary

The band-notched monopole ultra-wideband antenna using the square-looped resonator

or the end-coupled resonator has been presented. By using two resonators, the proposed antenna shows narrower notched bandwidth and good gain suppression ability in WLAN band. The set of parameter studies of the proposed antenna provides brief guidelines for the band-notched antenna design. Evaluations of return loss, radiation patterns, gain responses, and group delay confirm the antenna performance. These features of the proposed antenna demonstrate that the proposed antenna is suitable for UWB communicational applications and prevents interference from the WLAN system.



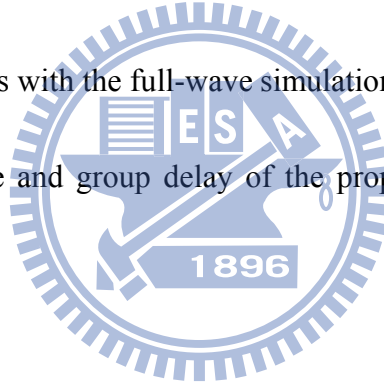
4 An UltraWideband Monopole Antenna with a Band-Notched Open-Looped Resonator

Previous literatures have mainly focused on the band-notched UWB antenna for wide operating bandwidth and band-notched performance. The band-notched performance in these literatures could utilize three observed criteria to estimate notched band antenna performance, i.e., gain suppression, bandwidth and roll-off rate (frequency selectivity) of the notched band. These criteria strongly relate to the structure and quality factor of the resonator. According to our knowledge and experiments, the resonator position at the antenna should be included in the notched-band antenna design because it is also related to band-notched performance. Hence, the quality factor and resonator position can be accommodated simultaneously to improve the controlled ability of the notched band.

To investigate band-notched performance, the proposed antenna consists of a fork-shaped antenna, an open-looped resonator with a high quality factor and two taped-lines. The fork-shaped antenna is designed for wide operating range. The proposed resonator is

placed at the center of the fork-shaped antenna, creating the 5-GHz notched band. Using this arrangement, this work emphasizes the resonator effects. The proposed antenna also shows good performance, such as fast roll-off rate of return loss, good gain suppression ability and narrow notched bandwidth at the notched band.

Section 4.1 presents the geometry and design concept of the proposed antenna and discusses important parameters for the fork-shaped antenna and band-notched performance. Section 4.2 shows the equivalent circuit model as a simple way to estimate the notched frequency of the proposed antenna. The calculated antenna input impedance using the proposed circuit mode agrees with the full-wave simulation data. Section 4.3 further examines the gain frequency response and group delay of the proposed antenna. Finally, section 4.4 draws conclusions.



4.1 Antenna Configuration and Performance

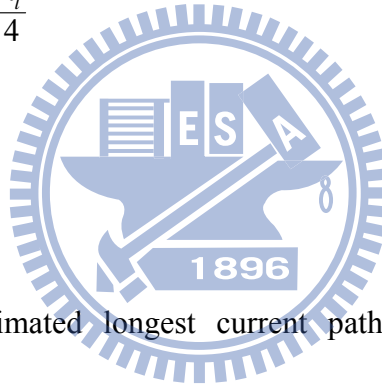
Figure 1 shows the geometry of the proposed antenna consisting of the fork-shaped antenna and the proposed resonator. The wide operating bandwidth of the fork-shaped antenna is mainly determined by three parameters, i.e., L_1 , L_2 and W_1 . The lowest frequency is determined by Eq. 4.1 to Eq. 4.3 and the tapered profile of the antenna structure is described by Eq. 4.4. α is the angle between the radiator and the ground plane.

$$f_l \approx \frac{c}{\sqrt{\epsilon_{eff}} \cdot L_l} \quad (4.1)$$

$$L_l = L_1 + \sqrt{L_2^2 + W_1^2} \approx \frac{\lambda_l}{4} \quad (4.2)$$

$$\epsilon_{eff} = \frac{\epsilon_r + 1}{2} \quad (4.3)$$

$$\alpha = \tan^{-1}(L_2 / W_1) \quad (4.4)$$



where L_l is the estimated longest current path along the outer radiating strip, approximated as a quarter of the length at the lowest frequency. The c and ϵ_{eff} are the speed of light and the approximated effective dielectric constant, respectively. The performance of the fork-shaped antenna at the UWB high band is related to α . Here, the UWB high band refers to the optional band from 5.85 to 10.65 GHz whereas the UWB low band represents the mandatory band from 3.1 to 5.1GHz [1],[21]. In our experiments, α should be 0.4-0.6 for better return loss level at the UWB high band.

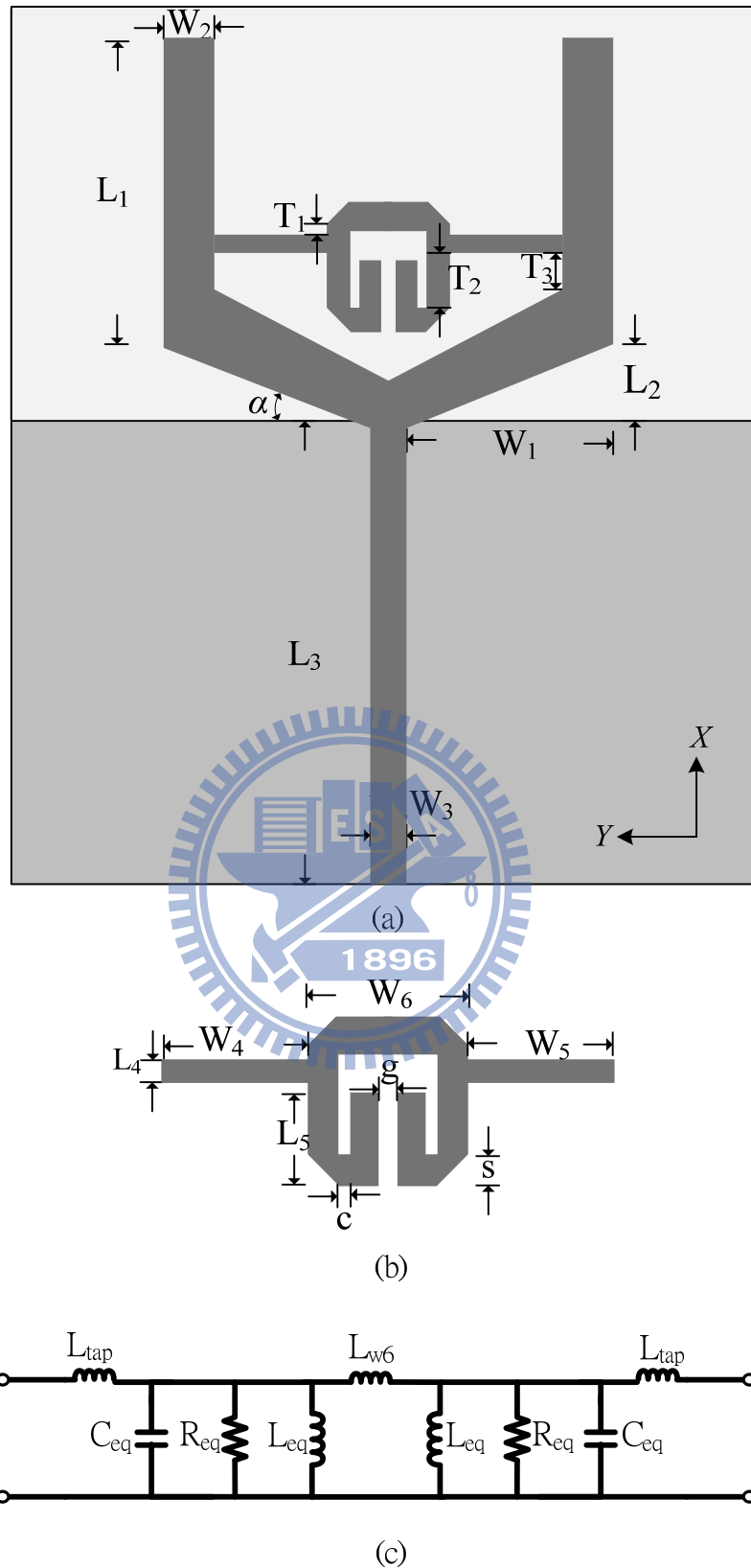


Fig. 4.1 Configuration of the proposed antenna. (a) Top view. (b) Proposed resonator. (c) Schematic equivalent circuit model of proposed resonator.

According to simulated current distributions of the planar monopole antenna, the current on the metal plate is inherently concentrated along the outer edges of the radiating plate, especially for the UWB low band. Based on this phenomenon, the resonator position at the interior of the antenna not only realizes a band-notched characteristic, but also preserves nearly the original characteristic of the antenna. The cutting triangular area, $0.5 \times 3.5 \text{ mm} \times 14 \text{ mm}$, is applied here to place the proposed resonator.

To achieve the band-notched property, the proposed resonator is symmetric around its centerline and consists of one open-looped resonator and two tapped lines as shown in Figure 4.1(b). The open-looped resonator is realized by folding back a half wavelength straight strip to form a pair of coupled lines. The coupled lines are connected together at one end. The total length of the coupled lines, $2 * L_5 + c$, approximates one-quarter wavelength. The current work uses the tapped-line to connect the proposed open-looped resonator and the fork-shaped antenna. The proposed resonator causes high input impedance level and impedance mismatching at the proposed antenna in the notched band.

Conceptually, the proposed resonator can be represented by the schematic equivalent circuit model shown in Fig. 4.1(c), in which each coupled line and the strip of W_6 can be represented by a lumped parallel lossy RLC circuit and inductive load, respectively. The tapped-line is treated as the inductive loads and capacitive loads. The capacitive coupling between two folded strips is ignored in Fig. 4.1(c). The resonant frequency of the proposed

resonator can be readily controlled by adjusting the equivalent inductance and capacitance values. It is noted that the proposed resonator is operated in inhomogeneous media without background plane. Thus, the proposed resonator neither supports the TEM mode nor forms the microstrip line resonator. Section 4.2 discusses the analysis and the simplified equivalent circuit model.

The antenna was fabricated on a 35 mm x 30 mm x 0.769 mm Rogers RO4350 substrate with dielectric constant $\epsilon_r = 3.48$ and loss tangent = 0.004 at 10 GHz. The final design parameters are $W_1 = 8.15$ mm, $W_2 = 2$ mm, $W_3 = 1.65$ mm, $W_4 = 4.5$ mm, $W_5 = 4.5$ mm, $W_6 = 5$ mm, $L_1 = 12.7$ mm, $L_2 = 3.3$ mm, $L_3 = 18$ mm, $L_4 = 0.4$ mm, $L_5 = 3$ mm, $T_1 = 0.4$ mm, $T_2 = 2.2$ mm, $T_3 = 1.5$ mm, $c = 0.3$ mm, $g = 0.4$ mm, $s = 1$ mm and $H = 0.769$ mm.

Figure 4.2 shows the simulated and measured return losses. The simulation was performed using Ansoft HFSS 9.2 while the measurement was taken by an Agilent E8362B performance network analyzer. The measured result agrees with the simulated result. The proposed resonator only slightly interferes with the return loss of the fork-shaped antenna except within the notched band. Figure 4.2 also shows the simulated result of the antenna without the proposed resonator, evidencing that the desired band notched property is introduced by the proposed resonator. The notched band reveals the narrow bandwidth and the fast roll-off rate due to the high quality factor and the appropriate position of the resonator.

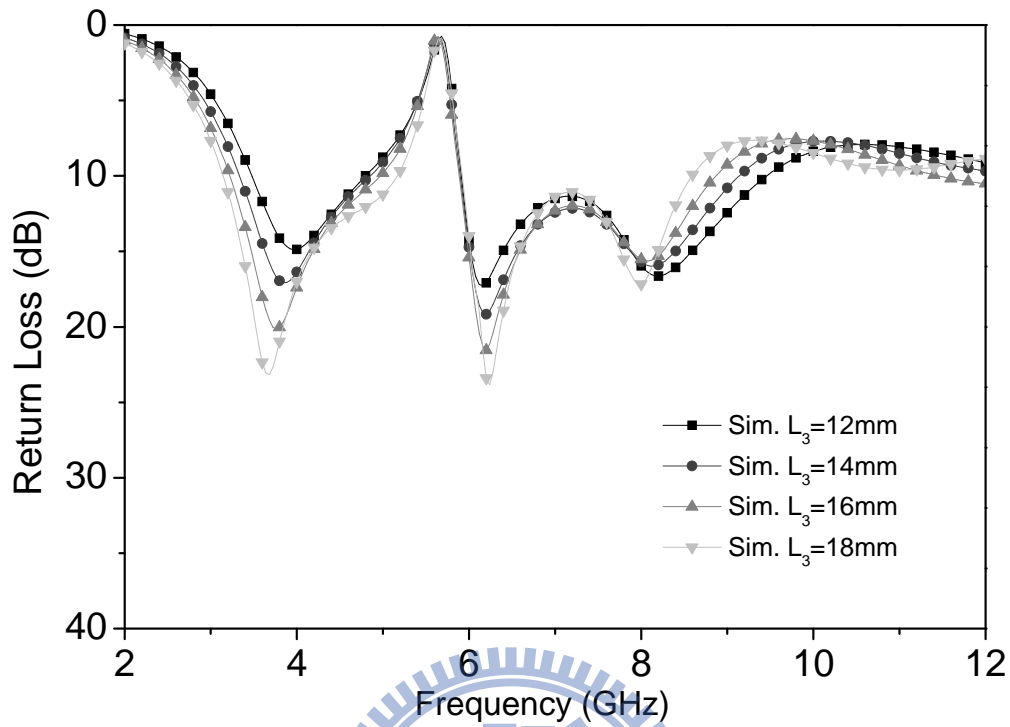


Fig. 4.3 Simulated return loss of various ground plane sizes.

In general, the ground plane can be treated as part of a small antenna. In this work, it is necessary to discuss the effect of the ground plane. Figure 4.3 shows the simulated return loss of various ground plane sizes. Observations show that the bandwidth of the UWB low band becomes significantly wider as L_3 changes from 12 mm to 18 mm but both the bandwidth of UWB high band and the return loss level of the notched band remain practically unchanged. According to this phenomenon, the larger ground size is proportional to the bandwidth at the UWB low band.

The antenna radiation patterns are measured in a 7.0m x 3.6m x 3.0m anechoic chamber

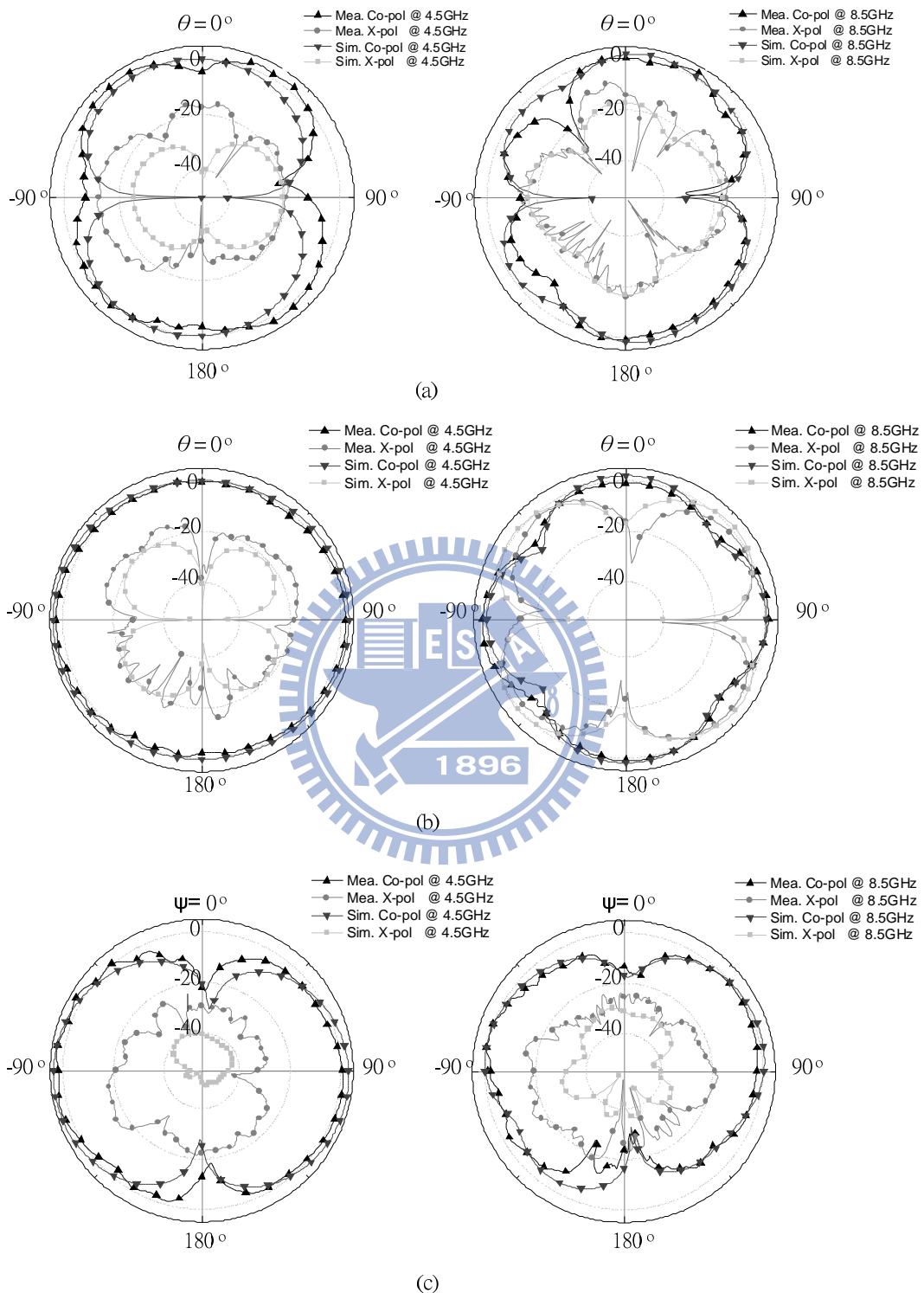


Fig. 4.4. Measured and Simulated radiation patterns at (a) xz-plane. (b) yz-plane. (c) xy-plane. (Unit:dBi)

with Agilent E8362B network analyzer as well as NSI2000 far-field measurement software.

Figure 4.4 shows the measured radiation patterns in yz-, xz- and xy-planes at 4.5 and 8.5 GHz. The measured patterns agree with the simulated patterns. Referring to Fig. 4.4(a), the co-polarization patterns are probably omni-directional shaped. The cross-polarization level rises considerably as frequency increases. The cross-polarization level is comparable to the co-polarization level in the yz-plane. In Figs. 4.4(b) and 4.4(c), the co-polarization patterns are the roughly dumbbell-like shaped and the cross-polarization levels are generally much lower than co-polarization levels. The discrepancies of cross-polarization in xy-plane and yz-plane can be attributed to the interference of the coaxial cable and the absorber.

4.2 Effect of Resonator on Notched Bands

To comprehend the effect of the proposed resonator, this subsection discusses the geometric parameters of the proposed resonator along with the fork-shaped antenna. The following discussions evaluate band-notched performance by the bandwidth, roll-off rate and return loss level of the notched band.

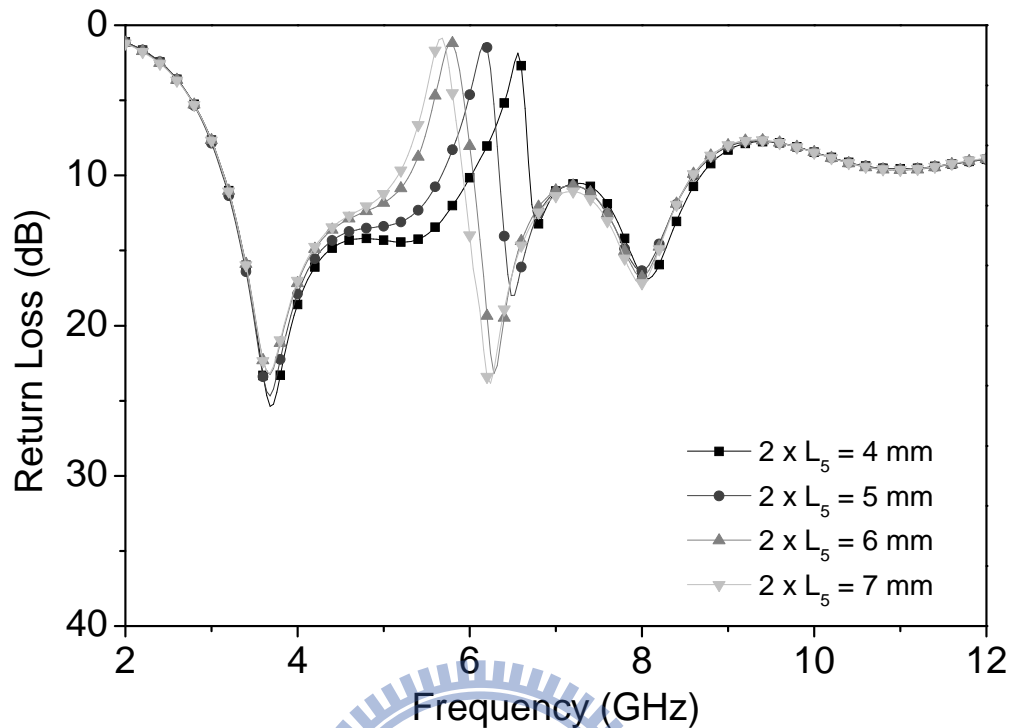


Fig. 4.5 Simulated return loss of various folded lengths of the resonator.

Figure 4.5 shows the simulated return loss of various folded lengths of the resonator.

The folded length of the open-looped resonator is the dominated element on the notched band.

As shown in Fig. 4.1(c), the folded length of the resonator, $2 * L_5 + c$, preliminarily

determines the values of the parallel RLC circuit. In the meantime, the resonant frequency of

the resonator is principally controlled by adjusting the values of the parallel RLC circuit. As

the folded strip length becomes longer, the amount of capacitive load of the parallel RLC

circuit increases accordingly. The center frequency of the notched band is simply in reverse

proportion to the folded length of the resonator. Simultaneously, the bandwidth and return

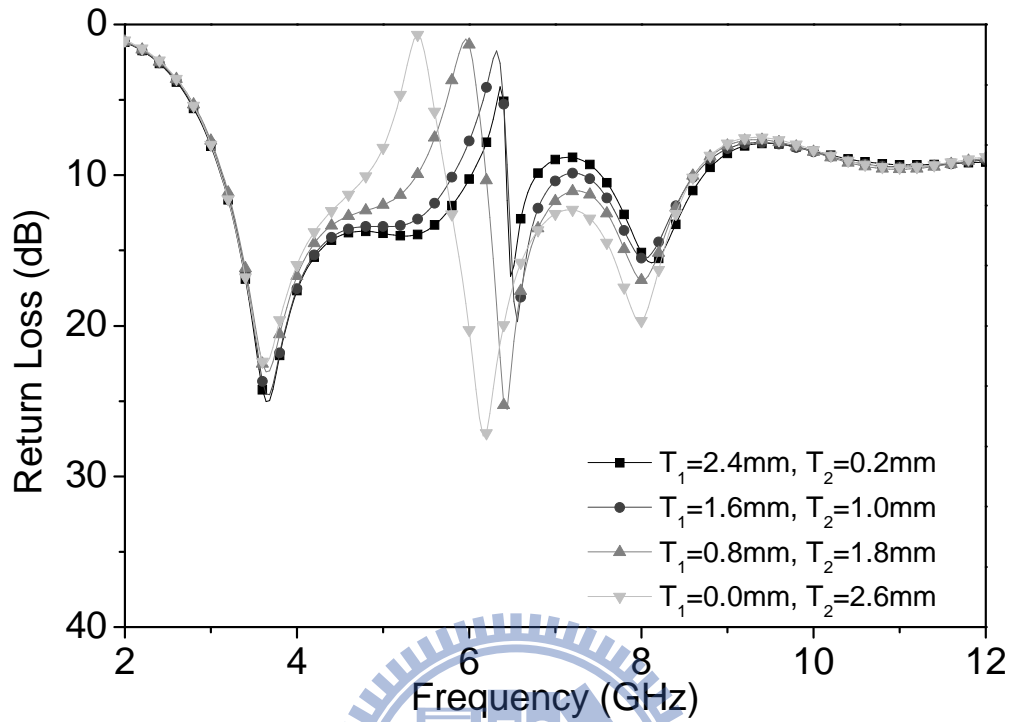


Fig. 4.6 Simulated return loss of various positions of the tapped-line.

loss level retain their original value.

Figure 4.6 shows the simulated return loss of various positions of the tapped-line. The position of the tapped line is the feeding input of the resonator. In this case, the position of the tapped-line moves vertically while the position of the whole open-looped resonator at the antenna is fixed. In this arrangement, the center notched frequency varies from 5.24 GHz to 6.46 GHz as T_1 and T_2 respectively changes from 0.0 and 2.6 mm to 2.4 and 0.2 mm at the fixed T_3 . The notched frequency shifts over a 1.2 GHz range as the tapped-line moves several millimeters. The result is different from the general filter design concept where the position of

the tapped-line cannot dominate the resonant frequency. To explain this phenomenon, the current study employed an equivalent circuit model of the resonator shown in section 4.3. According to the simulated results of the equivalent circuit model, the resonant frequency only shifts around 0.2GHz as the position of the tapped line changes in same condition. This implies a certain degree of dependency between the two situations, i.e., the resonator with ground plane and the resonator without ground plane. In the former situation, the resonator supports the quasi-TEM mode. Hence, the feeding position of the resonator cannot dominate the resonant frequency. In the latter situation, resonant frequency is easily influenced by changing the resonator input because the resonator is placed in the antenna/radiator without the ground plane.

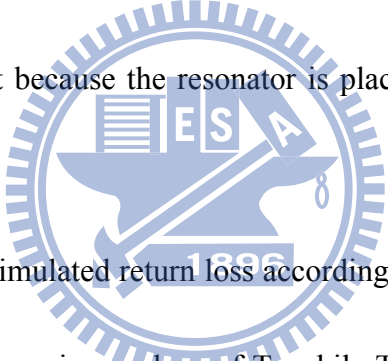


Figure 4.7 shows the simulated return loss according to various vertical positions of the resonator at the antenna, i.e., various values of T_3 while T_1 , T_2 , W_4 and W_5 are fixed. Here, the proposed resonator moves along the x-direction. The center frequency and the return loss level of the notched band slightly changes as T_3 changes from 1.8 mm to 7.8 mm, whereas the bandwidth of the notched band is significantly larger as the resonator is placed near the end of the fork-shaped antenna. In this case, since the proposed resonator structure is not changed, the unloaded quality factor of the proposed resonator or each component of Fig. 4.1(c) retains its original value. This study considers the external quality factor of the resonator when the resonator cooperates with the radiator/antenna. Figure 4.7 implies that when the resonator is

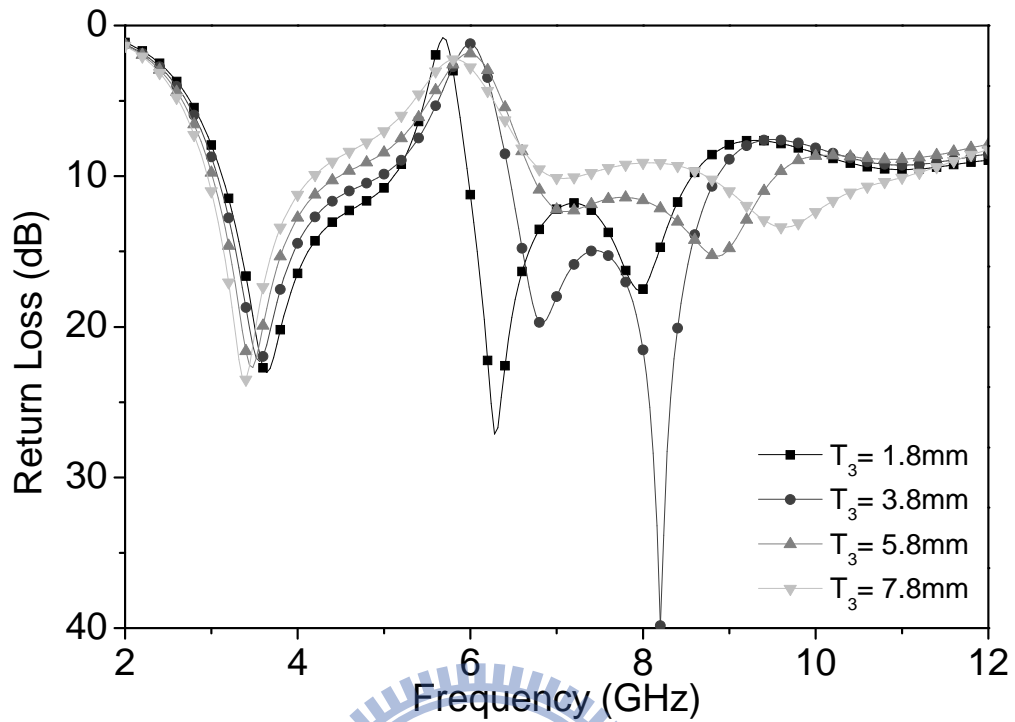


Fig. 4.7 Simulated return loss according to various vertical position of resonator at the antenna.

placed near the end of the fork-shaped antenna, the external quality factor becomes lower and the bandwidth of the notched band becomes wider simultaneously.

Figure 4.8 shows the simulated return loss according to horizontal positions of the resonator at the antenna, i.e., various values of W_4 and W_5 at fixed T_1 , T_2 and T_3 . Different from Fig. 4.7, the proposed resonator moves along the y -direction. Referring to Fig. 1(c), L_{tap1} is not equal to L_{tap2} because W_4 is not equal to W_5 . When the proposed antenna becomes non-symmetrical, the notched band moves farther apart and splits into two individual notched bands whose peak values are -1.2 dB at 5.56 GHz and -3.2 dB at 6.48 GHz when $W_4 = 2$ mm

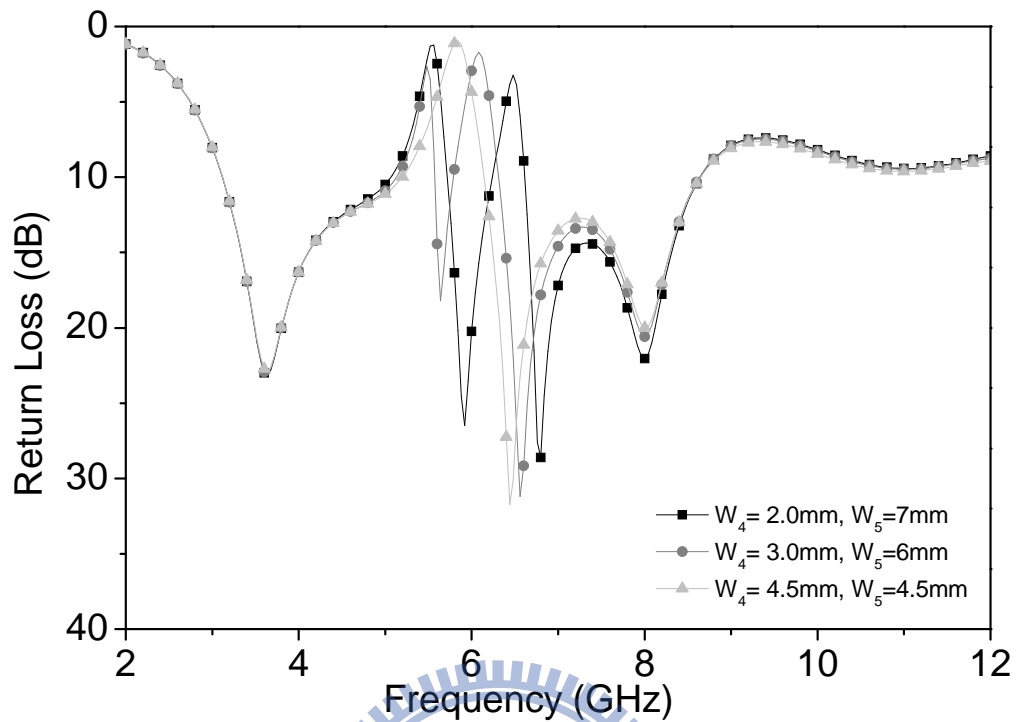


Fig. 4.8 Simulated return loss according to various horizontal positions of resonator at the antenna.

and $W_5 = 7$ mm, and are -2.91 dB at 5.4 GHz and -1.7 dB at 6.08 GHz when $W_4 = 3$ mm and $W_5 = 6$ mm, respectively. Figure 4.8 shows that the proposed resonator can be treated as two sub-resonators, where each sub-resonator is formed by a tapped-line and a folded strip of the open-looped resonator. The notched frequencies of the proposed antenna depend on the structure of each sub-resonator.

4.3 The Equivalent Circuit Model

Conceptually, the schematic equivalent circuit model shown in Fig. 4.1(c) represents the proposed resonator. The inductive and capacitive loads explain the band-notched behaviors at the notched band. However, it is difficult for band-notched antenna modeling using the schematic equivalent circuit model to obtain accurate values of each component. To tackle this problem, this section proposes the simplified equivalent circuit model to explain complex resonant behaviors.

This work first extracts the impedance characteristic of the proposed resonator shown in Fig. 4.9(a). Here, the dimension of each ground plane is 8 x 20 mm² and the two delta sources excite at each node interface of the proposed resonator at the Ref plane. The proposed resonator in the fork-shaped antenna is actually floating. Therefore, during the extracting process shown in Fig. 4.9(a), the proposed resonator is placed at the RO4350 substrate without ground plane to accompany the actual operating mechanism.

To transfer the proposed resonator to the equivalent lumped circuit model, the procedure of the equivalent lumped circuit model shown in Fig. 4.9(b) and 4.9(c) can be accounted for using the filter design theory in [22, Chap 6-8]. Using the HFSS simulation, the Z-parameters of the proposed resonator can be easily achieved and can transfer into a one-port lumped equivalent parallel resonant as shown in Fig 4.9(b) with

$$L_s = \frac{R_s}{2\pi f_c * Q_s} \quad (4.5)$$

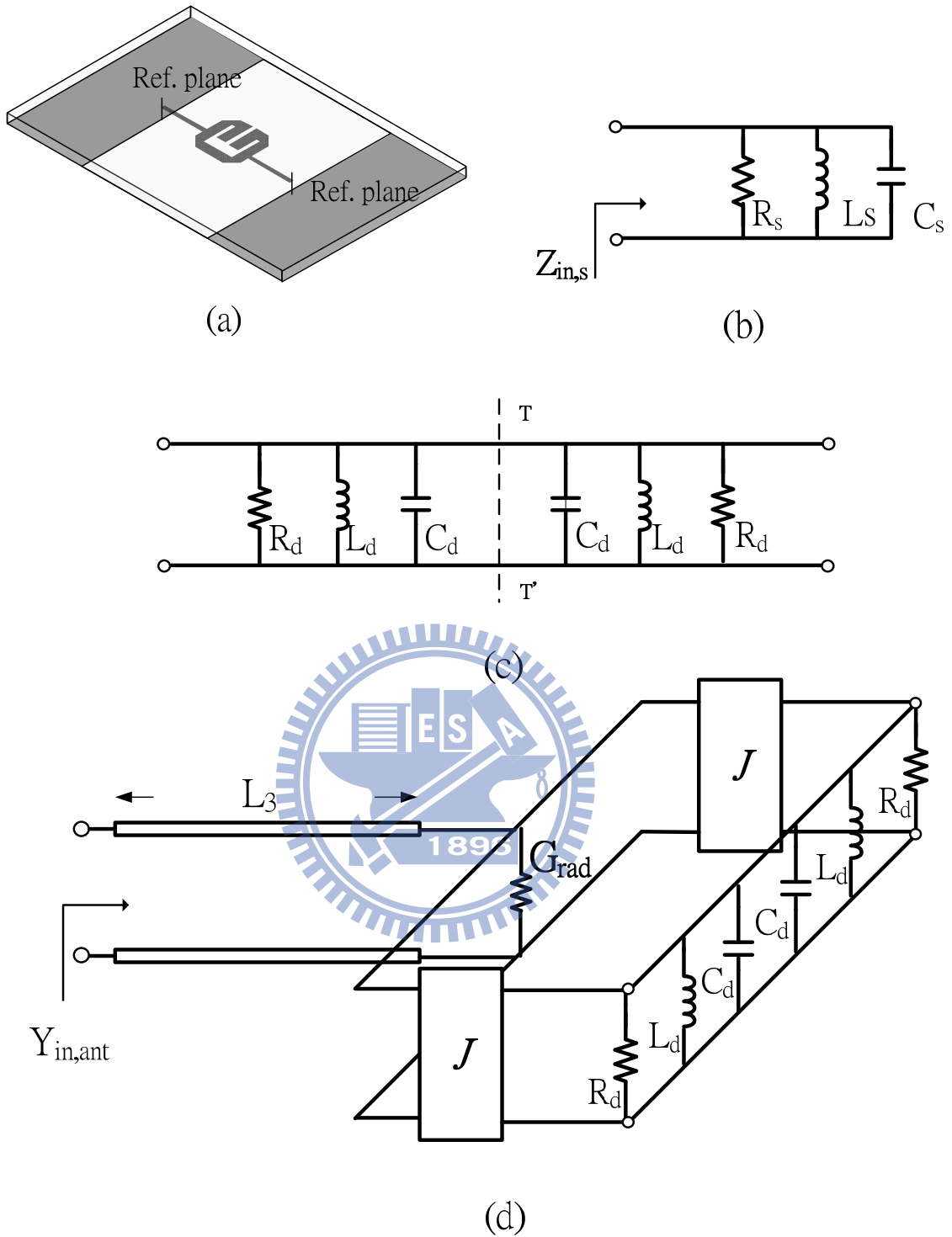


Fig. 4.9 (a) Exact structure of the proposed resonator. (b) One-port lump equivalent circuit network of the proposed resonator. (c) Two-port lump equivalent circuit network of the proposed resonator. (d) Simplified equivalent circuit model of the proposed antenna.

$$C_s = \frac{1}{(2\pi f_c)^2 L_s} \quad (4.6)$$

$$Q_s = \frac{f_c}{f_u - f_l} = \frac{1}{FBW} \quad (4.7)$$

FBW is the fractional bandwidth. f_u and f_l are frequencies as the input impedance magnitude of the one-port resonant network is respectively 0.707 times the maximum magnitude of the one-port network. f_c is the center resonant frequency of the resonator. R_s is the real part of the impedance of the one-port network at the center frequency. L_s and C_s are the inductance and capacitance of the one-port network, respectively. Because the resonator is symmetrical, the one-port resonant network can separate into the symmetrical two-port resonant network as shown in Fig. 4.9(c). The T-T' line is a symmetrical plane. Here, we define two-port network elements, Q_d , L_d , C_d and R_d , as

$$Q_d = \frac{Q_s}{2} \quad (4.8)$$

$$L_d = 2L_s \quad (4.9)$$

$$C_d = \frac{C_s}{2} \quad (4.10)$$

$$R_d = 2R_s \quad (4.11)$$

Note that R_d is the real part of impedance of the two-port network and is $2R_s$ to keep the real part of implement of the two-port network equal to that of the one-port network. R_s or R_d in the lumped circuit model represents the amount of conductor and dielectric loss, not radiation loss. Figure 4.9(c) presents the proposed resonator with two node interfaces by a two-port lumped circuit model.

In the modeling process, the metal strip is regarded as the high impedance line with a length of $T_3 + (W_1 + L_2)^{0.5}$, which is approximately one-quarter wavelength of the notched band. Here, the metal strip is between the proposed resonator and the feeding microstrip line. Hence, this metal strip behaves quite similarly to a quarter-wavelength transformer, and can be therefore modeled as a pair of J-inverters. The values of the J-inverter are determined by the characteristic admittance of the feeding microstrip line and the real-part admittance of the equivalent resonant circuit. G_{rad} stands for a constant radiation conductance and accounts for the wideband nature of the antenna. Finally, a simplified equivalent circuit model presents the proposed antenna as shown in Fig. 4.9(d). The extracted values of resonator parameters are summarized in Table 4.1 and $Y_{\text{in,ant}}$ is the input admittance of the antenna given by

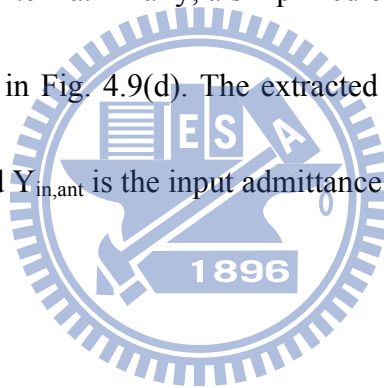


Table 4.1

Extracted values of the resonator parameters and J inverter

f_c	f_l	f_u
5.4GHz	5.24GHz	5.52GHz
R_d	C_d	L_d
1222ohm	0.467pF	1.85nH
Q_d	J-inverter	G_{rad}
9.64	0.057mho	0.02 mho

$$Y_{in,ant} = G_{rad} + \frac{2J^2}{\frac{1}{R_d} + j\omega C_d + \frac{1}{j\omega L_d}} \quad (4.12)$$

Figure 4.10 shows the simulated impedance of the proposed resonator and the simulated admittance of the proposed antenna, respectively. Reasonable agreement exists between the results of the HFSS simulation and the simplified equivalent circuit model. The discrepancy between the curves mostly attributes to the simplistic modeling of the resonator and the J-inverter. The results, in terms of a simplified equivalent circuit with higher quality factor, reasonably explain the narrower bandwidth of frequency gain response in section 4.3. Despite some inaccuracy in the simplified equivalent circuit model, the results still provide valuable information of antenna behavior.

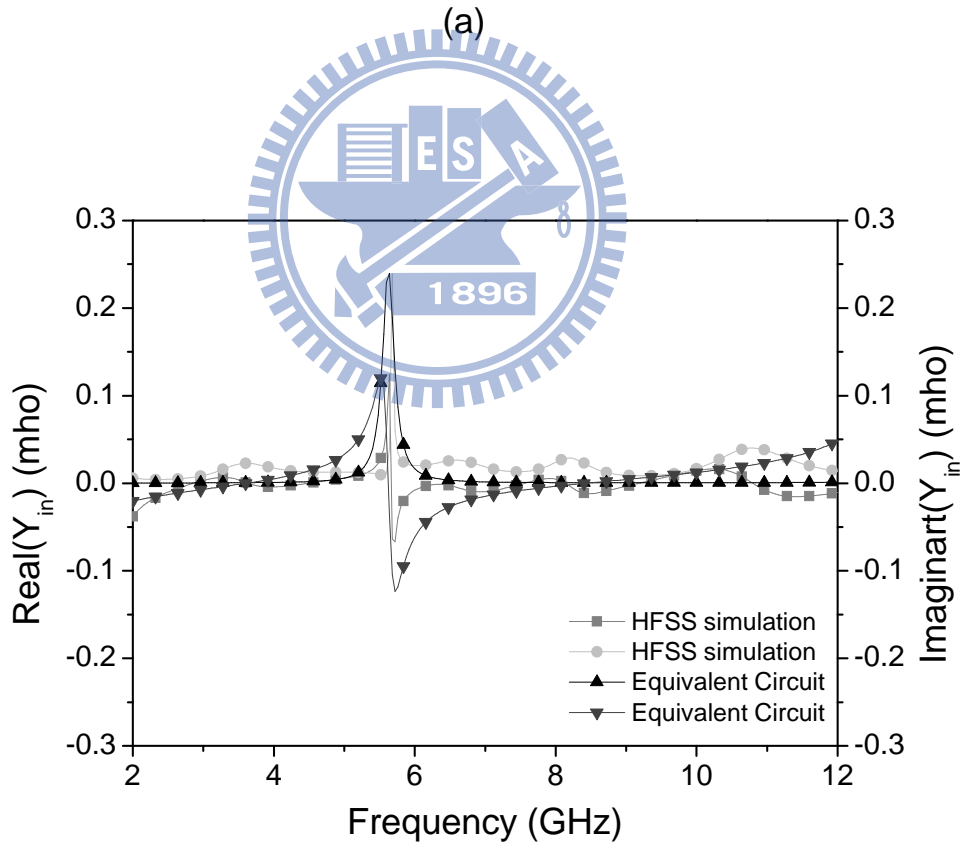
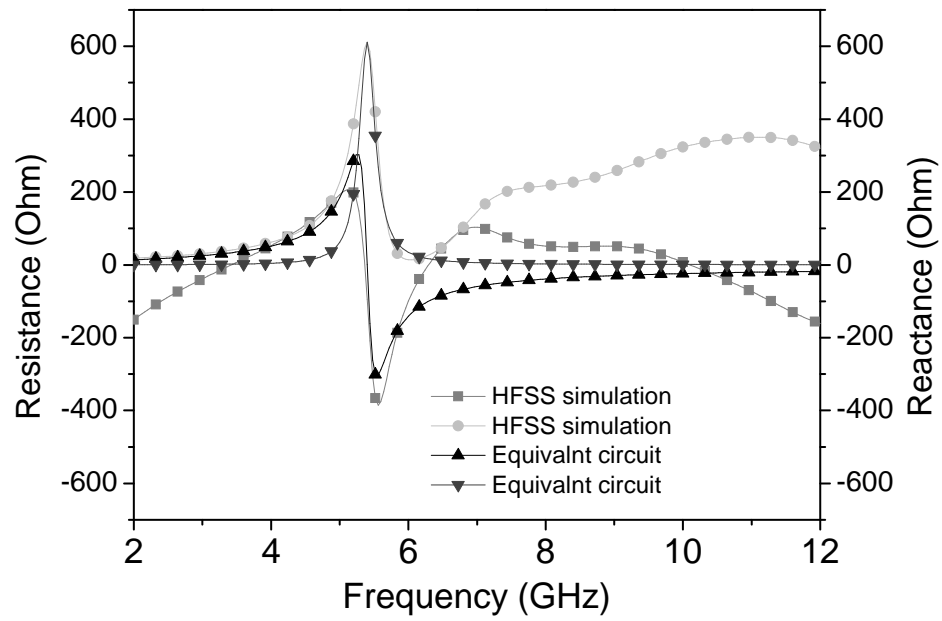
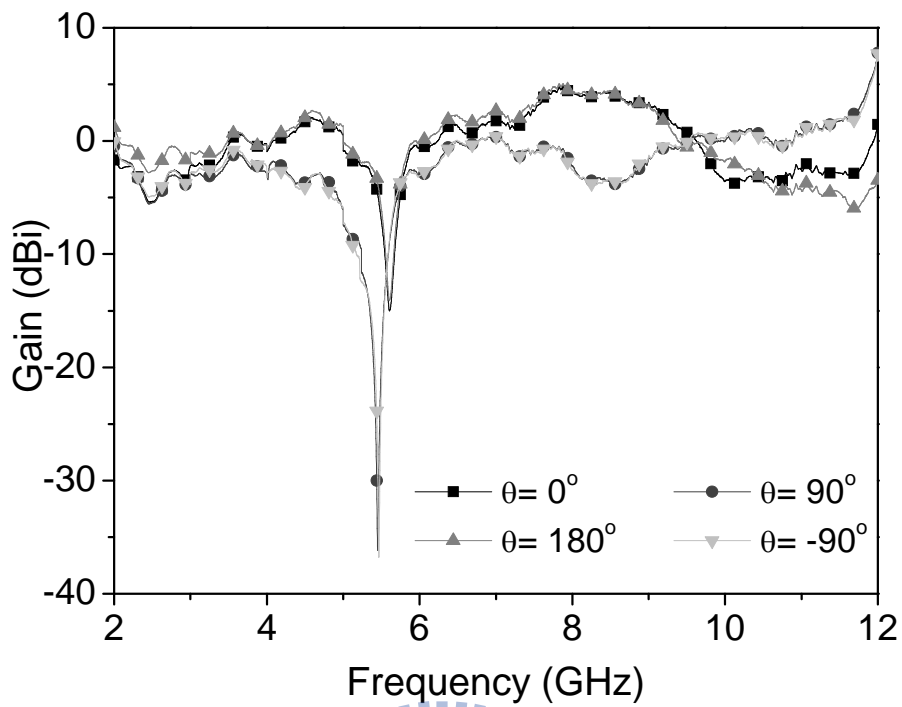


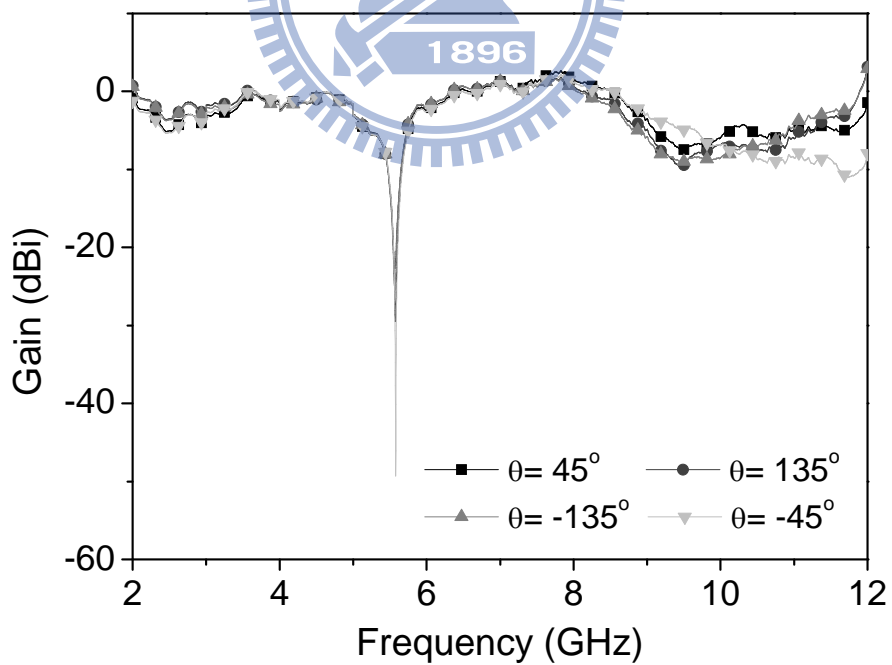
Fig. 4.10 Compared results between HFSS and the simplified equivalent circuit. (a) Simulated impedance of the resonator. (b) Simulated admittance of the proposed antenna.

4.4 Gain response and Group Delay

In measuring antenna gain frequency response, the EMCO 3115 double-ridge horn antenna with a constant group delay of 630 ps is used as a reference antenna for calibration. Figure 4.11 illustrates the measured gain frequency responses in the yz-plane at eight angles, ranged from -180° to 180° with 45° interval. The gain response of the proposed antenna is quite flat from 3.1 to 10.6 GHz except at the notched band. According to Fig. 4.11, the range of gain suppression is from 15 dB to 35 dB within these eight angles at the target notched band. Although the notched band slightly shifts at $\theta = 90^\circ$ and at $\theta = -90^\circ$, it remains within the range of the target notched band. The notched frequencies are quite similar at the observation angles. The notched bandwidth is significantly narrower due to the fast roll-off rate and high level of return loss at the notched band. The distance between the referenced antenna and the proposed antenna is 3.4 m. In the UWB system, the constant group delay response is required. Figure 4.12 presents the measured group delay of the proposed antenna. Except at the notched band, group delay variation over the 3.1 to 10.6 GHz is less than 130 ps with average of 718 ps as the spatial angle varies. Figures 4.11 and 4.12 show that the proposed antenna has good time/frequency characteristics and a small pulse distortion over the UWB operated band.



(a)



(b)

Fig. 4.11 Measured gain response of the proposed antenna. (a) $\theta = 0^\circ$, $\theta = 90^\circ$, $\theta = 180^\circ$, $\theta = -90^\circ$. (b) $\theta = 45^\circ$, $\theta = 135^\circ$, $\theta = -135^\circ$, $\theta = -45^\circ$.

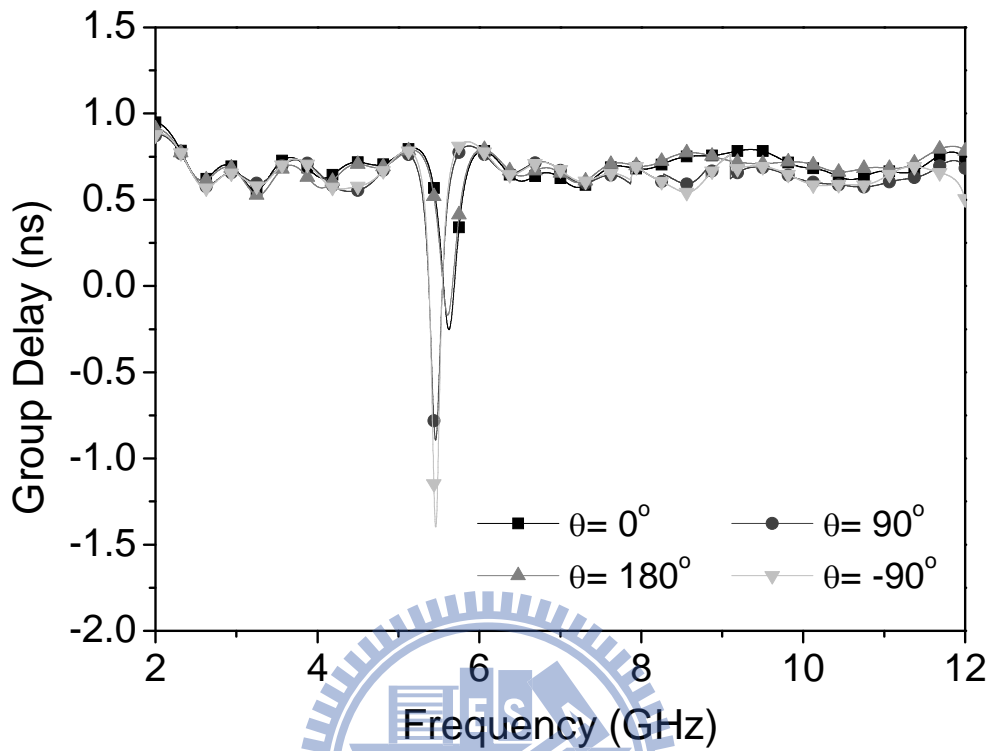
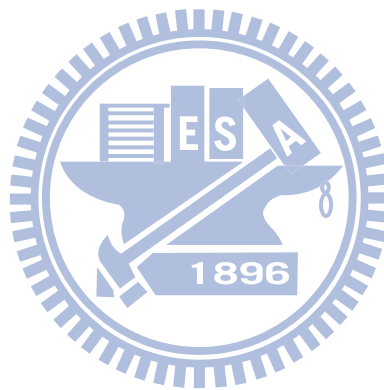


Fig. 4.12 Measured group delay of the proposed antenna.

4.5 Summary

This chapter proposes and analyzes a novel band-notched monopole ultra-wideband antenna. By applying an open-looped resonator, the antenna shows a narrower bandwidth and high return loss level as well as good gain suppression ability at the desired notched band. The parameter studies of the proposed antenna provide brief guidelines for a band-notched antenna design using the similar monopole antenna and resonator. This study investigates these parameters in terms of the relationship between the fork-shaped antenna and the

open-looped resonator. The simplified equivalent circuit model explains the rather complicated resonant behavior of the proposed antenna. The calculated antenna input admittance using the simplified equivalent circuit model agrees with the HFSS simulated result. Evaluations of return loss, radiation patterns, gain responses, and group delay confirm the antenna performance. These features of the proposed antenna demonstrate that the proposed antenna is suitable for UWB communicational applications and prevents interference from the WLAN system.



5 Conclusion

A novel category of band-notched UWB planar antenna with resonator structure has been demonstrated. A fork-shaped UWB antenna with a tapped-line coupled resonator, a square-looped resonator, an end-coupled resonator and an open-looped resonator respectively are presented. The circuit topology of impedance and dimensionless normalized antenna transfer function for analyzing an UWB antenna are discussed as well. More improvements and applications will be implemented in the future.

5.1 Conclusion

In this dissertation, the Forster canonical forms have been firstly proposed to describe the impedance of the UWB antenna and the band-notched UWB antenna. The dimensionless normalized antenna transfer function is then derived to describe the antenna frequency domain characterization. This transfer function eliminates the space effect in the transmitting-receiving antenna system. Cooperating with the traditional antenna parameters such as return loss, radiation patterns, a comprehensive picture of the UWB antenna characteristics can be obtained. Consequently, the band-notched UWB antenna planar monopole antenna with tapped-line coupled resonator is presented. The proposed antenna has shown band-notched performance due to the proper-positioned tapped-line coupled resonator at the fork-shaped antenna. The proposed antenna also features flat gain frequency response and 10 to 18dB gain suppression in the notched band. Compared to other UWB antennas, the proposed antenna demonstrates that it is suitable for UWB communicational applications and prevents interference from the WLAN system.

In chapter 3, the band-notched monopole ultra-wideband antenna using the square-looped and the end-coupled resonator has been presented. By using two resonators, the proposed antenna shows narrower notched bandwidth and good gain suppression ability at the desired notched band. The parameter study of the proposed antenna with square-looped resonator provides brief guidelines for the band-notched antenna design. Evaluations of return

loss, radiation patterns, gain responses, and group delay confirm the antenna performance.

Chapter 4 proposes and analyzes a novel band-notched monopole ultra-wideband antenna. By applying an open-looped resonator, the antenna shows a narrower bandwidth and high return loss level as well as good gain suppression ability at the desired notched band. The parameter studies of the proposed antenna provide brief guidelines for a band-notched antenna design using the similar monopole antenna and resonator. This study investigates these parameters in terms of the relationship between the fork-shaped antenna and the open-looped resonator. The simplified equivalent circuit model explains the rather complicated resonant behavior of the proposed antenna. The calculated antenna input admittance using the simplified equivalent circuit model agrees with the HFSS simulated result. Evaluations of return loss, radiation patterns, gain responses, and group delay confirm the antenna performance.

5.2 Future Work

Possible improvements on the antenna designs as well as on antenna modeling techniques are addressed as future work in this subchapter.

First of all, actually, two needed notched bands are 0.2 GHz for lower WLAN band and 0.1 GHz for upper WLAN band. However, most band-notched UWB antenna designs have only single notched band to cover two notched bands, because either the band-notched structure occupies a large space of the antenna or the strong couplings between two

band-notched structures are not easy eliminated. Besides, the some notched bandwidths occupy too much wide band-notch that reaches more than 1.5-2 GHz. Using the resonator structure provides a good solution. Through the resonator structure, the notched frequency and bandwidth can be readily achieved and improved in a limited space.

Secondly, the UWB devices with compact size and high performance are required in the UWB community. In such UWB system, the antenna should be the largest component to reach the miniaturization and to be integrated with circuit. The low temperature co-fire ceramics (LTCC) process will be a solution to tackle this issue. With the LTCC process, the antenna can be integrated with the circuit in a semiconductor chip or package. However, it should be noted that the radiation efficiency and radiation patterns may degrade.

Thirdly, the array and diversity techniques of antenna get more and more attentions in wireless communication. These techniques could be applied to UWB systems, for data transfer, imaging, localization, and radar applications.

Finally, in addition to utilizing the slot, the plastic slit, and the resonator to achieve band-notched performance, antenna with ground defected structure (GDS) would be of interest. Various design methods of the band-notched UWB antenna to achieve system requirement is worth investigating.

6 Reference

- [1] Task Group 3a Homepage, [Online]. Available: <http://www.ieee802.org/15/pub/TG3a.html>
- [2] UWB, Forum Homepage, [Online]. Available: <http://www.uwbforum.com>.
- [3] M.Z. Win, R.A. Scholtz and M.A. Barnes, "Ultra-wide bandwidth signal propagation for indoor wireless communications," *Communications, 1997. ICC 97 Montreal, Towards the Knowledge Millennium. 1997 IEEE International Conference on*, vol.1, no., pp.56-60 vol.1, 8-12 Jun 1997
- [4] Do-Hoon Kwon, "Effect of antenna gain and group delay variations on pulse-preserving capabilities of ultrawideband antennas," *IEEE Trans. Antennas Propag.*, vol.54, no.8, pp.2208-2215, Aug. 2006
- [5] T. G. Ma and S. J. Wu, "Ultrawideband band-notched U-shape folded monopole antenna and its radiation characteristics," *Ultra-Wideband Short Pulse Electromagnetics 8*, pp. 49-56, Springer Publisher, 2007.
- [6] C. Y. Hong, C. W. Ling, I. Y. Tran, and S. J. Chung, "Design of a planar ultrawideband antenna with a new band-notch structure," *IEEE Trans. Antennas Propag.*, vol. 55, no.12, pp. 3391-3397, Dec. 2007.
- [7] R. Zaker, C. Ghobadi and J. Nourinia, "Novel modified UWB planar monopole antenna with variable frequency band-notch function," *IEEE Antennas Wireless Propag. Lett.*, vol 7, pp. 112-114, 2008.
- [8] J. C. Young, H. K. ki, H. C. Dong, S. S. Lee and S. O. Park, "A miniature UWB planar monopole antenna with 5-GHz band-rejection filter and the time-domain characteristics," *IEEE Trans. Antennas Propag.*, vol.54, no.5, pp.1453-1460, May 2006.
- [9] K. Chawanonphithak, C. Phongcharoenpanich, S. Kosulvit and M. Krairiksh, "5.8 GHz Notched UWB Bidirectional Elliptical Ring Antenna Excited by Circular Monopole with Curved Slot," *Microwave Conference, 2007. APMC 2007. Asia-Pacific*, vol., no., pp.1-4, 11-14 Dec. 2007
- [10] Y. Yao, B. Huang and Z. Feng, "A Novel Ultra-Wideband Microstrip-Line Fed Wide-Slot Antenna Having Frequency Band-Notch Function," *Microwave and Millimeter Wave Technology, 2007. ICMMT '07. International Conference on*, vol., no., pp.1-4, 18-21 April 2007
- [11] C. S. Li and C. W. Chiu, "A CPW-fed band-notched slot antenna for UWB applications," *Antennas and Propagation Society International Symposium, 2008. AP-S 2008. IEEE*, vol., no., pp.1-4, 5-11 July 2008
- [12] J. S. McLean, H. Foltz, and R. Sutton, "Pattern descriptors for UWB antennas," *IEEE Trans. Antennas Propag.*, vol. 53, pp. 553-559, Jan. 2005.

- [13] S. B. T. Wang, A. M. Niknejad, and R. W. Brodersen, "Circuit modeling methodology for UWB omnidirectional small antennas," *IEEE J. Select. Areas Commun.*, vol. 24, no. 4, pp. 871–877, 2006.
- [14] A. M. Abbosh, and M. E. Bialkowski, "Design of ultrawideband planar monopole antennas of circular and elliptical shape," *IEEE Trans. Antennas Propag.*, vol. 56, no.1, pp. 17-23, Jan. 2008.
- [15] Z. N. Chen, T. S. P. See, and X. Qing, "Small printed ultrawideband antenna with reduced ground plane effect," *IEEE Trans. Antennas Propag.*, vol. 55, no 2, pp. 383-388, Feb. 2007.
- [16] C. Shi, P. Hallbjorner and A. Rydberg, "Printed slot planar inverted cone antenna for ultrawideband applications," *IEEE Antennas Wireless Propag. Lett.*, vol 7, pp.18-21, 2008.
- [17] T. G. Ma and S. K. Jeng, "Planar miniature tapered-slot-fed annular slot antennas for ultra-wideband radios," *IEEE Trans. Antennas Propag.*, Vol. 53, pp. 1194-1202, Mar. 2005.
- [18] X. N. Low, Z. N. Chen, and W. K. Toh, "Ultrawideband suspended plate antenna with enhance impedance and radiation performance," *IEEE Trans. Antennas Propag.*, vol. 56, no.8, pp. 2490-2495, Aug.2008.
- [19] C. D. Zhao, "Analysis on the properties of a coupled planar dipole UWB antenna," *IEEE Antennas Wireless Propag. Lett.*, vol 3, pp. 317-320, 2004.
- [20] S. Cheng; P. Hallbjorner, A. Rydberg, "Printed Slot Planar Inverted Cone Antenna for Ultrawideband Applications," *IEEE Antennas Wireless Propag. Lett.*, vol.7, no., pp.18-21, 2008
- [21] T. G. Ma; S. K. Jeng, "Planar miniature tapered-slot-fed annular slot antennas for ultrawide-band radios," *IEEE Trans. Antennas Propag.*, vol.53, no.3, pp. 1194-1202, March 2005
- [22] E. Gschwendtner and W. Wiesbeck, "Ultra-broadband car antennas for communications and navigation applications," *IEEE Trans. Antennas Propag.*, vol.51, no.8, pp. 2020-2027, Aug. 2003
- [23] Y. C. Lin and K. J. Hung, "Compact Ultrawideband Rectangular Aperture Antenna and Band-Notched Designs," *IEEE Trans. Antennas Propag.*, vol.54, no.11, pp.3075-3081, Nov. 2006
- [24] Z. N. Chen, Terence S. P. See and X. Qing, "Small Printed Ultrawideband Antenna With Reduced Ground Plane Effect," *IEEE Trans. Antennas Propag.*, vol.55, no.2, pp.383-388, Feb. 2007
- [25] S. G. Mao and S. L. Chen, "Frequency- and Time-Domain Characterizations of Ultrawideband Tapered Loop Antennas," *IEEE Trans. Antennas Propag.*, vol.55, no.12, pp.3698-3701, Dec. 2007
- [26] K. Chang, H. Kim and Y.J. Yoon, "Ultra-wideband antenna with improved gain characteristics," *IET Microw. Antennas Propag.*, , vol.2, no.5, pp.512-517, August 2008
- [27] C. S. Li and C. W. Chiu, "A CPW-fed band-notched slot antenna for UWB applications,"

- Antennas and Propagation Society International Symposium, 2008. AP-S 2008. IEEE*, vol., no., pp.1-4, 5-11 July 2008
- [28] S. Nikolaou, A. Amadjikpe, J. Papapolymerou, and M. M. Tentzeris, "Compact Ultra Wideband (UWB) Elliptical Monopole with Potentially Reconfigurable Band Rejection Characteristic," *Microwave Conference, 2007. APMC 2007. Asia-Pacific*, vol., no., pp.1-4, 11-14 Dec. 2007
- [29] J. Qiu, Z. Du, J. Lu, and K. Gong, "A planar monopole antenna design with band-notched characteristic," *IEEE Trans. Antennas Propag.*, vol. 54, no.1, pp. 288-292, Jan.2006.
- [30] W. S. Lee, W. G. Lim, and J. W. Yu, "Multiple band-notched planar monopole antenna for multiband wireless systems," *IEEE Microwave Wireless Compon. Lett.*, vol. 15, pp.576-578, Sep. 2005.
- [31] T. Dissanayake and K. P. Esselle, "Predication of the notch frequency of slot loaded printed UWB antennas," *IEEE Trans. Antennas Propag.*, vol. 55, no.11, pp. 3320-3325, Nov. 2007.
- [32] K. H. Kim, and S. O. Park, "Analysis of the small band-rejected antenna with the parasitic strip for UWB," *IEEE Trans. Antennas Propag.*, vol. 54, pp. 1688-1692, Jun. 2006.
- [33] S. W. Qu, J.L. Li and Q. Xue, "A Band-Notched Ultrawideband Printed Monopole Antenna," *IEEE Antennas Wireless Propag. Lett.*, vol.5, no.1, pp.495-498, Dec. 2006
- [34] H. Deng, X. He, B. Yao and Y. Zhou, "Compact band-notched UWB printed square-ring monopole antenna," *Antennas, Propagation and EM Theory, 2008. ISAPE 2008. 8th International Symposium on*, vol., no., pp.1-4, 2-5 Nov. 2008.
- [35] T. G. Ma and S. J. Wu, "Ultrawideband band-notched U-shape folded monopole antenna and its radiation characteristics," *Ultra-Wideband Short Pulse Electromagnetics 8*, pp. 49-56, Springer Publisher, 2007.
- [36] T. G. Ma and S. J. Wu, "Ultrawideband band-notched folded strip monopole antenna," *IEEE Trans. Antennas Propag.*, vol. 55, pp. 2473-2479, Sep. 2007.
- [37] B. Scheers, M. Acheroy, and A. V. Vorst, "Time-domain simulation and characterization of TEM horns using a normalize impulse response," *Proc. Inst. Elect. Eng. Microw. Antennas Propag.*, vol. 147, pp.463-468, Dec. 2000.
- [38] C. E. Baum, E. G. Farr, and C. A. Frost, "Transient gain of antennas related to traditional continuous-wave (CW) definition of gain," *Proc. Ultra-Wideband Short-Pulse Electromagnetics 4*, Jun. 1998, pp. 109-118
- [39] Jang, J.-W.; Hwang, H.-Y., "An Improved Band-Rejection UWB Antenna With Resonant Patches and a Slot," *IEEE Antennas Wireless Propag. Lett.*, vol.8, no., pp.299-302, 2009
- [40] T. G. Ma, R. C. Hua, and C. F. Chou, "Design of a multiresonator loaded band-rejected ultrawideband planar monopole antenna with controllable notched bandwidth," *IEEE Trans. Antennas Propag.*, vol. 56, no. 9, pp. 2875-2883, Sep. 2008.
- [41] K. Chung, J. Kim, and J. Choi, "Wideband microstrip-fed monopole antenna having

frequency band-notch function," *IEEE Microw. Wireless Compon. Lett.*, vol. 15, no. 11, pp. 766-768, Nov. 2005.

- [42] A. M. Abbosh, M. E. Bialkowski, and J. Mazierska, "A planar UWB antenna with signal rejection capability in the 4-6 GHz band," *IEEE Microw. Wireless Compon. Lett.*, vol. 16, no. 5, pp. 278-280, May 2006.

